THE EFFECTS OF THE POTENTIAL GLYCINE RECEPTOR ANTAGONIST, AMBD, IN THALAMIC VENTROBASAL NUCLEI

by

SARAH MONICA MCCARTHY

BSc., The University of Windsor, 2004

A THESIS SUBMITTED IN PARTIAL FULFILLMENT OF
THE REQUIREMENTS FOR THE DEGREE OF

MASTER OF SCIENCE

in

THE FACULTY OF GRADUATE STUDIES

(Pharmacology and Therapeutics)

THE UNIVERSITY OF BRITISH COLUMBIA

June 2006

ABSTRACT

This thesis describes the effects of 6-aminomethyl-3-methyl-4H,1,2,4-benzothiadiazine-1,1-dioxide (AMBD) on membrane properties and synaptic inhibition in neurons of the ventrobasal (VB) nuclei in the thalamus. Although gamma-aminobutyric acid (GABA) has a well-established role as a neurotransmitter in the VB nuclei, recent evidence demonstrates that this area exhibits glycinergic inhibition that is sensitive to blockade by strychnine. AMBD has pharmacological properties that are consistent with glycine receptor antagonism, but its actions in the thalamus are unknown.

The major objective was to determine the effects of AMBD on inhibitory postsynaptic currents (IPSCs) in the VB nuclei evoked by electrical stimulation of the medial lemniscus (ML), the major sensory input. AMBD significantly reduced the peak amplitude of glycinergic and GABA$_A$ergic mixed IPSCs, pharmacologically isolated glycinergic and GABA$_A$ergic IPSCs, and purely glycinergic IPSCs. AMBD had no effects on most of the purely GABA$_A$ergic IPSCs. AMBD eliminated the slow and intermediate, not the fast, decay components of mixed glycinergic and GABA$_A$ergic IPSCs. AMBD decreased the apparent frequency but not the amplitude of spontaneous IPSCs (sIPSCs), implicating a possible presynaptic action.

We propose that AMBD has both presynaptic and postsynaptic sites of action. According to this proposal, AMBD antagonized the effects of glycine-like amino acids at the postsynaptic fast and slow glycine receptors, as well as at a presynaptic site that attenuates the effects of GABA. Blockade of the presynaptic site resulted in reduced GABA release by nerve terminals. In summary, AMBD has actions expected from a specific antagonist of glycine-like amino acids at thalamic receptors.

TABLE OF CONTENTS

LIST OF TABLES

LIST OF FIGURES

ACKNOWLEDGEMENTS

My supervisor Dr. Ernie Puil, has made this MSc. such a wonderful experience. I have learned so much from Dr. Puil, both academically and personally. Thank you. I would also like to thank Dr. David Mathers for his suggestions and counsel throughout my studies. You have been so helpful. Thank you to my committee members, Dr. Bernie MacLeod and Dr. Craig Ries for their support and suggestions.

Thank you to Viktoriya Dobrovinska and Mr. Christian Caritey for their excellent technical assistance with my research. I would also like to thank Miti Isbasescu for his computer assistance. Thank you to Amer Ghavanini for his continual direction and patience everyday.

A special thank you to Stephanie Lee, who has made this experience unforgettable. I am so appreciative of her friendship, both in research and outside. I came into this degree looking for an education. I am leaving with a best friend for life. Thank you.

Thank you to CIHR and NSERC for financially supporting this work.

Thank you to Chris Bauer for his support everyday. You make my life so much better.

Finally, a huge thanks to my family. I have been able to study because of your continual support, throughout all of my lifetime. I dedicate this work to my parents, who have provided me with the confidence to pursue my dreams, whatever they may be.

Chapter I. Introduction

1.1 Scope of the thesis

This thesis describes the effects of a potential glycine antagonist, 6-aminomethyl-3-methyl-4H,1,2,4-benzothiadiazine-1,1-dioxide (AMBD, TAG), on neurons in the ventrobasal (VB) nuclei of the thalamus. In this thesis, we will refer to this substance as AMBD because its name in much literature, 'TAG', infers that it is a specific taurine antagonist. Although gamma-aminobutyric acid (GABA) has a well-established role as a neurotransmitter in the VB nuclei, recent evidence demonstrates that this area exhibits synaptic inhibition sensitive to blockade by strychnine (Ghavanini et al., 2005). Because strychnine antagonizes receptors for glycine-like amino acids, glycine, taurine or β-alanine, individually or in combination, may mediate this inhibition. Although AMBD has pharmacological properties that are consistent with glycine receptor antagonism, its actions in the thalamus have not been investigated. The major objective of this thesis was to investigate the synaptic effects of AMBD on inhibitory postsynaptic currents (IPSCs) in the VB nuclei. Based on previous literature, the general hypothesis was that AMBD interacted with synaptic glycine receptors and not GABA receptors, suppressing the inhibitory effects of glycine and β–amino acids. Minimal effects on $GABA_A$ergic responses might be interpreted as selectivity in AMBD action at the glycine receptor or a hypothetical receptor for β–amino acids.

1.2 Background

1.2.1 The ventrobasal nuclei of the thalamus

The VB nuclei complex consists of the ventral posterior medial (VPM) and ventral posterior lateral (VPL) nuclei (Jones, 1991). These nuclei relay information from somatic sensory receptors to cortical layers 1 to 6 of somatosensory neocortex (Brodman areas 1, 2, 3a and 3b; Feldman and Kruger, 1980). VB nuclei neurons are organized into subpopulations with axons that project to only one cortical layer, or multiple layers by collaterals (Manson, 1969; Jones, 1991). Corticothalamic neurons in layer 6 project back to the VB nuclei, producing excitatory and inhibitory inputs, potentially for receptive field adjustment (Alitto and Usrey, 2003). The ML provides the major sensory pathway to the brain and is a major input to the VB nuclei (Mountcastle et al., 1963).

The two major types of neurons identified in the thalamus are numerous thalamocortical (TC) relay neurons and a small population of local circuit interneurons (Yen and Jones, 1983). TC relay neurons can be distinguished from interneurons by somatic size and dendritic pattern. TC relay neurons have large somata and short radiating dendrites, whereas interneurons have small, round somata and extensive dendritic arborization (Yen et al., 1985; Turner et al., 1997). In addition, interneurons have more depolarized resting membrane potentials and lack the ability to fire at high frequencies above 150 Hz (Turner et al., 1997).

TC relay neurons are further subdivided into two major classes called Type I and II. Type I TC neurons are common, whereas Type II TC neurons are rare. Type I TC

neurons are morphologically characterized by large somata, large tufted dendrites, no appendages and thick axons. These neurons are further characterized by low input resistance (R_i), small afterhyperpolarizations and transient responses to current injection. Type I TC neurons project to cortical layers 4 and 5. Type II TC neurons are morphologically characterized by small somata, thin branching dendrites, thin appendages and thin axons. They are also characterized by high R_i, large afterhyperpolarizations and non-adapting responses to current injection. Type II TC neurons project to cortical layers 1 and 2 (Yen et al., 1985; Hirai and Jones, 1988; Jones, 1991; Turner et al., 1997). Investigations in the VB nuclei predominantly involve Type I TC neurons due to the small number of interneurons and Type II TC neurons in the rat (Harris and Hendrickson, 1987).

TC neurons that receive input from cortical layer 5 are further classified as higher-order thalamic relays, whereas those that receive input from other cortical layers are termed first-order relays (Guillery and Sherman, 2002). Higher-order TC neurons are involved in complex functions such as attention and are sensitive to cortical inactivation. First-order TC relay neurons are not affected by cortical inactivation and are involved in information transfer only (Diamond et al., 1992; Ward et al., 2002; Bokor et al., 2005).

The nuclei of the VB thalamus are the major thalamic relay centres for somatosensory information. VB nuclei are also involved in sleep and wakefulness cycles (Steriade, 2005), or pathophysiologically in absence epilepsy (Huguenard and Prince, 1994). Most inputs to the VB nuclei are contralateral and somatotopically organized (Waite, 1973;

Welker, 1973). VB neurons receive inputs from nociceptive and thermal spinal cord afferents by way of the spinothalamic pathway. They also receive information about touch, pressure and vibration peripheral afferents by way of the ML tract (Welker, 1973; Akers and Killackey, 1979; Feldman and Kruger, 1980; Jones, 1991). The ML is an excitatory and inhibitory input (Mountcastle et al., 1963; Hirai and Jones, 1988), whereas inputs from the nucleus reticularis (nRt) and zona incerta are only inhibitory (Peschanski et al., 1983; Bartho et al., 2002). In addition, the VB nuclei receive cholinergic and noradrenergic neuromodulatory inputs from the brainstem and basal forebrain (Castro-Alamancos and Calcagnotto, 2001).

1.2.2 Inhibitory neurotransmission in the VB nuclei

In the VB nuclei, inhibitory neurotransmission is mediated by GABA through predominantly postsynaptic $GABA_A$ and $GABA_B$ receptors and glycine-like amino acids through glycine receptors. $GABA_C$ receptors are not apparent in pharmacological studies of some thalamic nuclei (Wan and Puil, 2002). $GABA_A$ and glycine receptors are members of the pentameric ligand-gated ion channel superfamily. $GABA_A$ and glycine receptor activation results in Cl^- influx, causing postsynaptic inhibition due to hyperpolarization of the neuron away from the firing threshold and shunting of excitatory synaptic inputs (Ries and Puil, 1999; Lynch, 2004). Recent studies have shown that the co-release and co-transmission of glycine and GABA by glycinergic and $GABA_A$ergic pathways are more common than previously assumed. In the spinal cord, GABA and glycine are co-released from the same nerve terminal in vesicles containing both neurotransmitters (Chaudhry et al., 1998; Jonas et al., 1998). Furthermore, GABA and

glycine may have a common presynaptic vesicular transporter (Dumoulin et al., 1999). Postsynaptically, the $GABA_A$ and glycine receptors are co-localized, poised for co-release or co-transmission (Bohlhalter et al., 1994). Activation of postsynaptic glycine receptors inhibits $GABA_A$ receptors through a phosphorylation mechanism (Li et al., 2003).

1.2.2.1 GABA$_A$ergic inhibition

The $GABA_A$ receptor is comprised of five subunits forming a Cl^- channel (Johnston, 1996). There are currently 19 known $GABA_A$ receptor subunit isoforms: α_{1-6}, β_{1-3}, γ_{1-3}, δ_1, ε, θ, π and ρ_{1-3} (Nayeem et al., 1994; Simon et al., 2004). $GABA_A$ receptors are highly heterogenous because of the large number of subunit isoforms that combine to form functional receptors (Macdonald and Olsen, 1994). The major endogenous agonist of the $GABA_A$ receptor is GABA, but imidazole-4-acetic acid, taurine, β-alanine and gamma-amino beta-hydroxybutyric acid (GABOB) can also bind to a non-functional form of the receptor (Johnston, 1996). Binding of GABA to the $GABA_A$ receptor results in opening of the Cl^- channel and movement of the membrane potential towards the Cl^- equilibrium potential (E_{Cl}), causing hyperpolarization or depolarization. $GABA_B$ receptor activation contributes to slow inhibitory transmission and is metabotropic (Bowery, 1989). The $GABA_A$–mediated process contributes to most fast inhibitory transmission in the thalamus (Kaila, 1994).

1.2.2.2 GABA$_A$ receptor antagonists

There are several known antagonists of the GABA$_A$ receptor, including picrotoxin, bicuculline and gabazine. Picrotoxin, a mixture of picrotoxinin and picrotin, blocks the Cl⁻ channel, and hence antagonizes glycine receptors at concentrations higher than 10 μM (Lynch et al., 1995). Bicuculline is a potent competitive antagonist at GABA$_A$ receptors. This antagonist binds to low affinity GABA binding sites on the α subunits (Maksay and Ticku, 1984; Sigel et al., 1992). Bicuculline is specific for GABA$_A$ receptors up until a maximum concentration of 50 μM. Beyond 50 μM, bicuculline antagonizes glycine receptors in hippocampal neurons (Shirasaki et al., 1991). Gabazine (SR-95531) is a competitive antagonist of GABA$_A$ receptors, and is approximately equipotent with bicuculline (Michaud et al., 1986). In contrast to bicuculline, however, gabazine preferentially binds to high affinity GABA binding sites, potentially indicating higher specificity (Heaulme et al., 1986). Gabazine is specific to GABA$_A$ receptors up to a maximum concentration of 10 μM (Mori et al., 2002). In VB neurons, bicuculline and gabazine show approximately the same degree of specificity for the GABA$_A$ receptor (Ghavanini et al., 2005).

1.2.2.3 Glycinergic inhibition

The glycine receptor has a well-established action in inhibitory neurotransmission in the spinal cord and brainstem (Werman et al., 1968; Grillner et al., 1998). The evidence for glycinergic transmission in the thalamus is based on immunocytochemistry and pharmacological effects. Glycine (Rampon et al., 1996), glycine receptors (Araki et al., 1988), glycine receptor subunits (Ghavanini et al., 2005), glycine transporter 2 (Jursky

and Nelson, 1995) and strychnine binding sites (Zarbin et al., 1981; Frostholm and Rotter, 1985) have been demonstrated in the thalamus. Furthermore, stimulation of the ML activates IPSCs that are sensitive to blockade by strychnine in neurons of the VB nuclei (Ghavanini et al., 2005).

The glycine receptor is a pentameric Cl^- channel composed of α and β subunits forming an ion-conducting pore (Lynch, 2004). The α subunit has four isoforms (α_{1-4}) and is required for ligand-binding (Ruiz-Gomez et al., 1990). The β subunit interacts with gephyrin to anchor the synaptic receptor to the cell cytoskeleton (Kirsch and Betz, 1995). In the spinal cord, glycine receptors are predominantly α_2 homomers during development and become $\alpha_1\beta$ heteromers during adulthood (Malosio et al., 1991). Four extracellular domains (A-D) located on the glycine receptor amino terminal have been proposed to form an agonist-binding pocket (Rajendra et al., 1995; Vafa et al., 1999; Corringer et al., 2000).

Activation of the glycine receptor results in the opening of a Cl^- channel and movement of the membrane potential towards E_{Cl}. The glycine receptor is inhibitory during adulthood when E_{Cl} is more negative than membrane potential (Lynch, 2004). During development, neurons can have a high intracellular Cl^- concentration, resulting in glycine-mediated depolarizing excitation (Ito and Cherubini, 1991). The increase in Cl^- channel conductance produces most of the inhibition. A shunt of excitatory synaptic voltage can occur, depending on its location relative to the regions of spike generation (Ries and Puil, 1999).

In the spinal cord, glycine receptors are activated by glycine, taurine, β–alanine and D- or

L-serine (Tokutomi et al., 1989) in the following order of potency: glycine > β-alanine >

taurine >> serine (Figure 1.1) (Curtis et al., 1968). D- and L-serine have little or no

effect on VB neurons (Ghavanini et al., 2005). Glycine binds to loop A, Ile93, Ala101

and Asn102 in the glycine receptor agonist-binding pocket (Vafa et al., 1999). The β-

amino acids bind to loop A, in the Ala101-Thr112 region of the glycine receptor agonist-

binding pocket (Han et al., 2001). The β–amino acid binding site is thus structurally

close to, but distinct from, the glycine binding site. In VB nuclei, application of β-amino

acids causes an increase in conductance (Ghavanini et al., 2005).
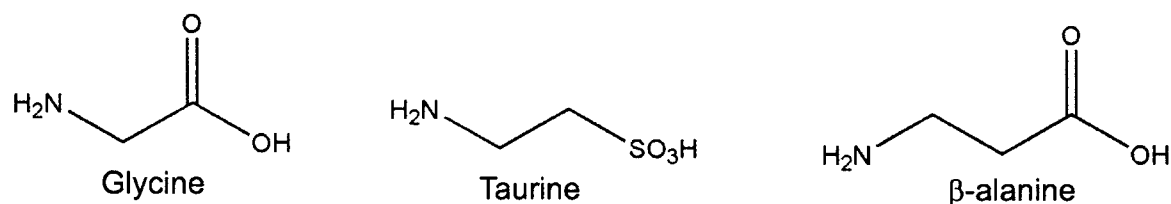
Figure 1.1 The chemical structures of the glycine receptor agonists, glycine, taurine and
β–alanine.

In the developing nervous system, taurine is abundant, particularly in the cerebellum,

thalamus and cerebral cortex (Curtis et al., 1971; Huxtable, 1989). It is implicated in

cortical plasticity, neuroprotection and inhibition of hyperexcitable states (Kaczmarek,

1976; Huxtable, 1989; Zhao et al., 1999). Taurine is proposed as a potential inhibitory

neurotransmitter due in part to its strychnine-sensitive actions on spinal neurons (Curtis et

al., 1968; Padjen et al., 1989). Taurine as a neurotransmitter is controversial because

Na^+-independent binding has not been demonstrated. Na^+-independent binding

demonstrates binding to the receptor rather than binding to membrane transporters (Huxtable, 1989). Although there are suggestions of a taurine-specific receptor, it has not been characterized (reviewed by Huxtable, 1989; Frosini et al., 2003).

1.2.2.4 Glycine and β–amino acid transporters

Glycine is transported from the extracellular space into the cytosol through two Na^+/Cl^- dependent glycine transporters (GlyT1 and GlyT2) (Eulenberg et al., 2005). GlyT1 transports $2Na^+/Cl^-$/glycine per cycle in glial cells. GlyT2 transports $3Na^+/Cl^-$/glycine per cycle on the presynaptic terminals of glycinergic neurons (Jursky and Nelson, 1995; Roux and Supplisson, 2000), and hence implicates glycinergic synapses. Immunocytochemistry for GlyT2 has demonstrated glycinergic synapses in the VB nuclei (Zeilhofer et al., 2005). The actions of GlyT1 and GlyT2 are antagonized by sarcosine and amoxapine, respectively (Nunez et al., 2000; Harsing et al., 2003).

There are two distinct transporters (TAUT1 and TAUT2) for the uptake of β–amino acids from the extracellular space (Liu et al., 1992; Smith et al., 1992). The TAUTs transport $2Na^+/Cl^-$/β-amino acid per cycle and are antagonized by guanidinoethane sulfonate (GES) (Huxtable et al., 1979; Nelson, 1998; Barakat et al., 2002). The 12 transmembrane segments of the TAUTs share significant homology with the glycine transporters (Liu et al., 1992). Although not localized to the thalamus, immunocytochemical staining for the TAUTs has been demonstrated throughout the brain, particularly in the cerebellum, cortex and hippocampus (Pow et al., 2002).

1.2.2.5 Glycine receptor antagonists

The two principal antagonists of the glycine receptor are strychnine and picrotoxinin.

Strychnine is the only established selective antagonist of the glycine receptor (Figure 1.2)

(Legendre, 2001). Other substances, such as brucine alkaloids, block glycine actions but

have not received extensive investigation presumably because they are much less potent

than strychnine (Curtis et al., 1968). In the hippocampus, strychnine is specific at

concentrations up to 2 μM, beyond which it also blocks GABA$_A$ receptors (Shirasaki et

al., 1991). Glycine and strychnine do not act at the same binding site, but there may be

some site overlap on the N terminal region of the glycine receptor α subunit (Graham et

al., 1983). Although picrotoxinin is a glycine receptor antagonist, it is less specific and

less potent than strychnine and also antagonizes GABA$_A$ receptors (Lynch et al., 1995).

The β subunit of the glycine receptor is involved in the effects of picrotoxin (Bormann et

al., 1993).
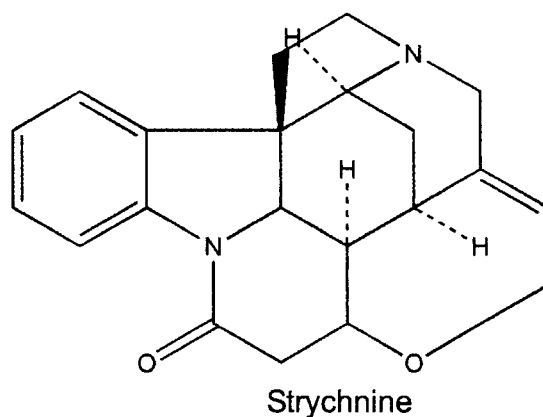
Strychnine

Figure 1.2 The chemical structure of the glycine receptor antagonist, strychnine.

1.2.3 AMBD: A potential β–amino acid antagonist

In 1982, Girard et al. discovered that 6-aminomethyl-3-methyl-4H,1,2,4-

benzothiadiazine-1,1-dioxide (AMBD) (Figure 1.3) acted as a taurine antagonist, but the

results of subsequent studies have been ambiguous. Although most studies have

indicated that AMBD is specific for the effects of β–amino acids, some investigations

have concluded that it also antagonizes the actions of glycine and GABA (Yarbrough et

al., 1981; Okamoto et al., 1983; Mathers, 1993). AMBD is a 1,2,4-benzothiadiazine

compound with an acidic centre and basic nitrogens in a rigid and planar conformation.

The distance between the acidic centre and basic nitrogens closely resembles GABA,

glycine, taurine and β-alanine (Girard et al., 1982). Although the distance between the

acidic and basic groups of taurine is less than AMBD, rotation of the aminomethyl group

toward C-5 may produce a closer structural match, resulting in a taurine-specific effect

(Girard et al., 1982; Huxtable et al., 1987). Comparisons between AMBD and taurine

indicate structural similarity but the exact AMBD binding site remains unresolved.

Girard et al. (1982) proposed that receptors recognize the sulfonamide group on AMBD

due to its structural similarity to taurine.
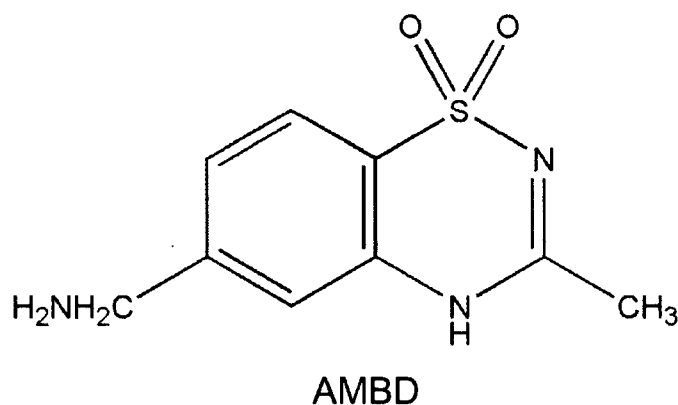
AMBD

Figure 1.3 The chemical structure of the potential β–amino acid antagonist AMBD.

1.2.3.1 The actions of AMBD on non-thalamic neurons

Studies employing ionophoretic application techniques indicate that AMBD specifically antagonizes the inhibitory effects of β–amino acids, with minimal action on either glycine or GABA-induced effects. Ionophoretic application of AMBD on rat and pig cerebellar and spinal neurons *in-vivo* antagonized taurine- and β–alanine-induced depolarization depression with minimal effects on GABA- or glycine-induced responses (Yarbrough et al., 1981; Girard et al., 1982; Okamoto et al., 1983; Billard and Batini, 1991). In terms of receptor specificity, these results are difficult to interpret because the concentration of ionophoretically applied AMBD is unknown.

Studies employing non-ionophoretic experimental techniques also indicate AMBD specificity for β–amino acids. In isolated frog spinal cord, bath application of 0.1-0.25 mM AMBD to dorsal root terminals selectively blocked taurine-induced responses with no effects on GABA- or glycine- induced responses (Padjen et al., 1989). In the rat substantia nigra, microinjection of AMBD antagonized contraversive turning evoked by taurine injection but had no effects on the binding of GABA to anxiolytic binding sites (Martin et al., 1981). In whole rabbit brain homogenate, 500 μM AMBD displaced [^{3}H]taurine with no effects on the GABA$_A$ agonists [^{3}H]muscimol or [^{3}H]GABA (Frosini et al., 2003). In whole rat brain homogenate, 250 μM AMBD reduced uptake of taurine and [^{3}H]taurine, with no effects on GABA or [^{3}H]GABA uptake (Lewin et al., 1994).

Most research on AMBD indicates specificity for β–amino acids but a few studies suggest otherwise. Application of 250 μM AMBD to dissociated salamander retinal cells

caused blockade of both taurine- and glycine-induced currents (Pan and Slaughter, 1995). These results are not necessarily applicable to the VB nuclei because the retina has more specialized neurotransmission compared with other CNS areas (Bormann, 2000). In dissociated mouse spinal cord neurons AMBD exhibited a narrow concentration range for taurine specificity (Mathers, 1993). In homogenized mouse cerebral cortex slices, application of 1 mM AMBD attenuated stimulated taurine release (Kontro and Oja, 1987), suggesting a presynaptic action of AMBD. In dissociated ventromedial hypothalamic neurons, bath application of 10^{-5} M AMBD had no effects on glycine or taurine-induced Cl⁻ currents (Tokutomi et al., 1989). The lack of effect suggests this concentration was too low for this particular system.

Past research on the action of AMBD has demonstrated specific antagonism of the effects of β–amino acids within a narrow concentration range which varies depending on the system under investigation. This specificity has been demonstrated, using ionophoretic and other techniques, in the cerebellum, spinal cord and substantia nigra of the rat, rabbit, mouse, frog and pig. Differing experimental techniques may explain the contradictory results. For example, high concentrations may have been responsible for some effects observed after ionophoretic application where the drug concentration is unknown. Further research using quantitative drug delivery techniques is required to resolve these issues.

1.3 Experimental rationale, objectives and hypothesis

The recent demonstration of strychnine-sensitive transmission in the VB nuclei is surprising because of the well-established role of GABA in this area. The inhibitory action of β-amino acids in the VB nuclei suggests that transmission mediated by the glycine receptor may involve more neurotransmitters than glycine alone (Ghavanini et al., 2005). Glycinergic inhibition may result from co-transmission or co-release, of combinations of glycine, taurine and β-alanine. The controversy around the action of AMBD could be resolved by demonstration of different glycine receptor binding sites or different receptors for the β-amino acids and glycine. Hence, demonstration that AMBD specifically blocks β-amino acids would be consistent with the hypothesis of differing binding sites or receptors. Therefore, we were interested in determining the effects of AMBD on the multi-transmitter system in the VB nuclei and whether the action of AMBD resembled strychnine which antagonizes glycine-like amino acids. Resolution of these issues may allow further identification of the neurotransmitters involved in VB nuclei IPSCs antagonized by strychnine, but not bicuculline.

The objective was to assess with patch clamp the concentration-dependent effects of AMBD on intrinsic, membrane and synaptic properties of individual thalamic neurons. For determining the specificity of AMBD, IPSCs were evoked by stimulation in the ML and pharmacologically identified as $GABA_A$ergic, glycinergic or mixed $GABA_A$ergic and glycinergic. Glycinergic IPSCs may have resulted from the receptor actions of glycine, taurine or β-alanine. The effects of AMBD on IPSCs were assessed from changes in peak IPSC amplitude, rise time, decay time and decay time constants. The effects of

AMBD on neuronal membrane properties were also investigated. This thesis examined the possibility that AMBD acted on synaptic receptors to specifically antagonize the action of glycine–like amino acids, with minimal effects on GABA-mediated transmission.

Chapter II. Materials and Methods

2.1 Whole-cell patch clamp recording

2.1.1 Slice preparation

All experiments were approved by the University of British Columbia Committee on Animal Care. Sprague-Dawley rats (12-14 days old) were placed under a gas-tight inverted glass funnel and anesthetized with halothane. Rats were decapitated after approximately 1 minute of deep anesthesia. The brain was rapidly removed and quickly submerged in ice-cold (4 °C), oxygenated (95% O_2 : 5% CO_2) artificial cerebrospinal fluid (aCSF) containing (in mM): 124 NaCl, 26 $NaHCO_3$, 1.25 NaH_2PO_4, 2.5 KCl, 2 $MgCl_2$, 2 $CaCl_2$, and 10 dextrose, at pH 7.3-7.4. The brain was sectioned along the interhemispheric fissure into two identical tissue blocks. The medial surface of the block was glued to the Teflon stage of a Vibroslicer (Campden Instruments Ltd., London, England). Parasagittal slices (200-250 μm thick), containing the VB nuclei and ML were cut. Slices were maintained for 1.5 hours on a polypropylene mesh in a holding chamber containing oxygenated aCSF (23-25 °C) at pH 7.3-7.4. The average osmolarity was 315 ± 1.0 mOsm.

2.1.2 Electrophysiological recording

Recording pipettes were drawn from borosilicate glass tubing with internal filament (World Precision Instruments, Sarasota, USA) using a vertical electrode puller (Narishige Instruments, Tokyo, Japan). For recording of IPSCs, pipettes were filled with an intracellular solution containing (in mM): 140 K-gluconate, 5 KCl, 4 NaCl, 3 $MgCl_2$, 1 $CaCl_2$, 10 EGTA, 1 HEPES, 3 MgATP, 0.3 Na_2GTP. Under these conditions, E_{Cl} was

-53 mV and E_K was –84 mV, when intracellular $[Ca^{2+}]$ was approximately 5 nM (calculated using Max Chelator software). The pH was adjusted to 7.3-7.4 using 50% gluconic acid and KOH. The average osmolarity was 252 ± 2.0 mOsm. For recording of spontaneous IPSCs (sIPSCs) the intracellular solution contained (in mM): 16.5 Cs-gluconate, 128.5 CsCl, 4 NaCl, 3 $MgCl_2$, 1 $CaCl_2$, 10 EGTA, 10 HEPES, 3 MgATP, 0.3 Na_2GTP, 3 QX-314. Under these conditions, E_{Cl} was 0 mV. The pH was adjusted to 7.3-7.4 using 50% gluconic acid and CsOH. Adenosine triphosphate (ATP) and guanosine triphosphate (GTP) were added to the pipette solution immediately prior to recording. Electrode resistances ranged between 5 and 10 MΩ.

After 1-2 hours incubation in aCSF, slices were placed in a Perspex chamber with volume of 1.5-2 ml. Slices were immobilized using a polypropylene mesh and perfused with bubbled (95% O_2 and 5% CO_2) aCSF with 1 mM kynurenate (23-25 °C) at a rate of 2 ml/minute. Kynurenate was used to block ionotropic glutamatergic transmission and isolate IPSCs (cf. Ghavanini et al., 2005). The VB nuclei and ML were visually identified using differential interference contrast (DIC) microscopy at 400x magnification (Axioscope, Carl Zeiss, Germany).

Whole cell patch clamp recording was performed using a List EPC-7 (HEKA, Lambrecht, Germany) in the voltage-clamp or current-clamp mode. Signals were filtered at 3 kHz, digitized at 10 kHz with a 16-bit data acquisition system (Axon Instruments) and stored for later analysis using pClamp software (Axon Instruments) on a Pentium computer. Neurons were accepted for further study if they had stable membrane

potentials and responded to depolarizing current pulse injections with overshooting action potentials.

IPSCs were evoked from a bipolar tungsten electrode (World Precision Instruments) connected to an isolated stimulator (Digitimer, Hertfordshire, UK). The electrode was placed in the ML, approximately 3 mm from the recording electrode. Stimuli at < 0.5 Hz with single pulses of duration 0.05 - 1 ms were employed and adjusted for maximal IPSC responses. 10 IPSCs were evoked for each treatment. Stimuli remained constant for single neurons throughout the procedure. Neurons were held at −80 mV for all IPSC experiments.

To identify the acting inhibitory neurotransmitter, IPSCs were characterized using 2 μM strychnine and 20 μM bicuculline to isolate the glycinergic and $GABA_A$ergic components, respectively. More than 95% inhibition of the IPSC by strychnine or bicuculline indicated purely glycinergic or purely $GABA_A$ergic responses. Partial blockade of an IPSC by either antagonists indicated mixed glycinergic or $GABA_A$ergic responses. Percentage inhibition of IPSC amplitude was calculated to quantify inhibition by AMBD, strychnine and bicuculline. Percentage inhibition was measured by calculating the percentage of original IPSC amplitude that was inhibited after application of an antagonist.

2.2 Drugs

Stock solutions were prepared in distilled water or dimethyl sulfoxide (DMSO) and diluted in aCSF. Drugs for IPSC experiments were applied by bath perfusion for ~ 8 minutes at 2 ml/min. All drugs applied to the slice were previously oxygenated. Bicuculline methiodide, strychnine and kynurenate were purchased from Sigma Chemical Company (St. Louis, USA). The first batch of AMBD was a kind gift of Merck Frosst Company (Montreal, Quebec, Canada) and the second batch was synthesized by BioFine International (Vancouver, BC, Canada). All drugs were washed out after application. Complete recovery was defined as 25% IPSC inhibition or less.

2.3 Data analysis

Electrophysiological data analysis was conducted using pClamp (Clampfit, Axon Instruments), Microsoft Excel and CorelDraw (Ottawa, Canada) software. Membrane potential was adjusted for a junction potential of -11 mV. R_i and membrane time constant (τ_m) were calculated from < 5 mV voltage responses to hyperpolarizing injections of current. Voltage-current relationships were determined from voltage responses to depolarizing and hyperpolarizing intracellular injections of current from -150 pA to 150 pA in neurons held at -60 mV. Tetrodotoxin (TTX) was not used in voltage-current experiments, so the recorded reversals may include presynaptic and Na^+-dependent contributions. Reversal potentials were obtained from the intersection of the control and drug curves.

2.3.1 IPSC analysis

After aligning current peaks in time, traces of 10 successive IPSCs from each treatment protocol were averaged for analysis. Rise time of the IPSC was determined by measuring the time between the initial deflection of the baseline current and peak IPSC amplitude. Charge transfer was determined by measuring the area under the IPSC. The decay phases of the averaged IPSCs were fitted with exponential functions to determine decay time constants. The single exponential function was,

$$y = Ae^{-t/\tau}$$

where A was the peak amplitude and τ was the decay time constant. The double exponential function was,

$$y = A_1 e^{-t/\tau_1} + A_2 e^{-t/\tau_2}$$

where A_1 and A_2 were the peak amplitudes of the terms with fast and slow time constants τ_1 and τ_2.

2.3.2 sIPSC detection and analysis

pClamp software template search was used to detect sIPSCs using a sliding template procedure. The sIPSCs recorded in the VB thalamus have 3 distinct time courses; fast sIPSCs decay within 100 ms, intermediate sIPSCs decay within 100-200 ms and slow sIPSCs decay within 500-1000 ms (cf. Ghavanini et al., 2006). Based on this finding, short, intermediate and slow sIPSC templates were produced using averaged sIPSCs that were visually detected. Detection threshold was set at 5 pA and all accepted events were visually monitored.

2.3.3 Concentration-response analysis

A concentration-response relationship for AMBD antagonism of the IPSC was established using cumulative drug application in a step-wise manner. Sigmoid curves were fitted to the data using Prism GraphPad software (San Diego, USA). The fitting equation for the single sigmoid relationship was,

$$y = \frac{\text{Max Response}}{(1 + IC_{50} - [\text{drug}])^n}$$

where max response was the plateau response, IC_{50} was the concentration at half-maximal response and n was the slope of the sigmoid curve.

2.3.4 Statistical analysis

All data were expressed as mean ± SEM and n denoted the number of neurons tested. Data were statistically analyzed using the NCSS Statistical Analysis System (Kaysville, USA). The Student's t-test was used for comparing two groups and the analysis of variance (ANOVA) was used for multiple comparisons. Significance was defined as $P < 0.05$.

Chapter III. Results

3.1 Chemical similarity of AMBD obtained from two sources

We used three spectroscopic methods for analysis of 6-aminomethyl-3-methyl-4H,1,2,4-benzothiadiazine-1,1-dioxide (AMBD or TAG) obtained from Merck and Biofine (cf. Methods). Ultraviolet (UV) spectrum absorbance peaks, high-pressure liquid chromatography (HPLC) absorbance peaks and proton nuclear magnetic resonance (NMR) spikes were identified and compared to determine if AMBD manufactured by the two sources were identical. No substantial differences were noted between the sources (Figure 3.1). Minor differences were likely attributable to salt preparation (cf. Kirkpatrick and Sandberg, 1973). The results of analysis with UV, HPLC and NMR techniques provided confirmation of the identity of AMBD from the two sources.

3.2 Effects of AMBD on membrane properties

Before observing the effects of AMBD on synaptic inhibition, it was necessary to determine if AMBD (250 µM) had effects on membrane properties that might account for its proposed antagonism. Initially, the 250 µM concentration of AMBD was chosen based on previous research that determined that this concentration specifically antagonized taurine when bath applied to neurons (Mathers, 1993). We assessed the effects of AMBD on membrane potential (V_m), R_i, τ_m, action potential firing, voltage-current relationships and baseline current. AMBD was applied to 19 previously untreated neurons, 19 bicuculline (20 µM) pre-treated neurons and 19 strychnine (2 µM) pre-treated neurons. Strychnine and bicuculline were co-applied after AMBD treatment. The average V_m for all neurons was -52 ± 1.5 mV (n = 39).
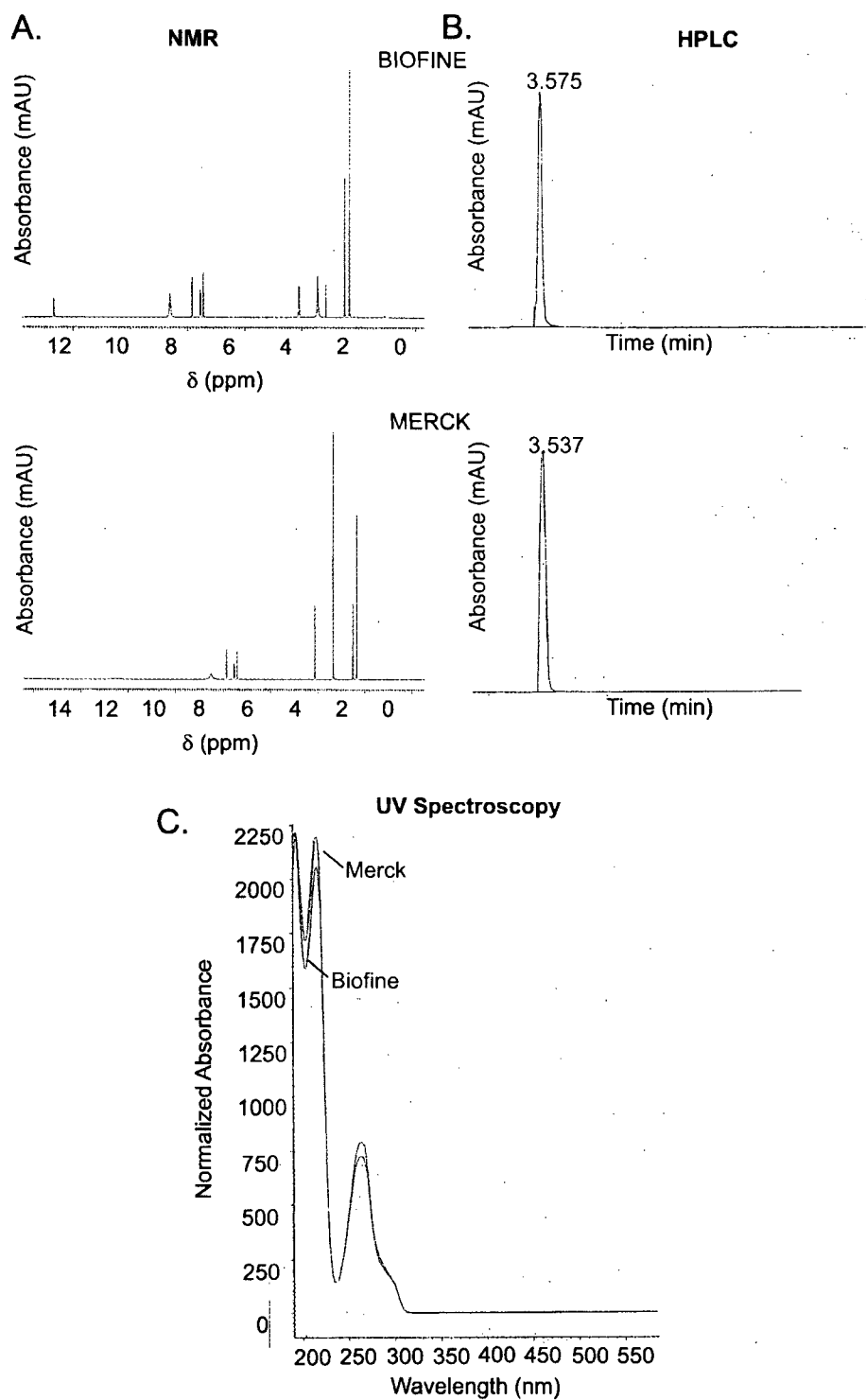
Figure 3.1 Three spectroscopic techniques confirmed the similar nature of AMBD obtained from two sources. (A) NMR absorbances of the two substances were a close match. Note slightly differing δ axes. (B) HPLC peaks for the two sources of AMBD closely matched eachother. (C) Overlapping UV absorbances also closely matched.

3.2.1 Input resistance and membrane time constant

We assessed the effects of AMBD (250 μM) on R_i and τ_m. Input capacitance was

calculated using R_i and τ_m measurements. Average R_i of neurons in control solutions was

323 ± 44 MΩ and the average τ_m was 41 ± 6 ms (n =19). The average input capacitance

of neurons was 130 ± 10 pF (n = 19).

Application of AMBD had no significant effects on R_i of previously untreated (n = 19),

bicuculline (20 μM) pre-treated (n = 19) or strychnine (2 μM) pre-treated (n = 19)

neurons (paired *t*-test, P > 0.05). AMBD also had no significant effects on input

capacitance of previously untreated (n = 19), bicuculline (20 μM) pre-treated (n = 19) or

strychnine (2 μM) pre-treated (n = 19) neurons (paired *t*-test, P > 0.05) (Table 3.1).

Hence, AMBD had no significant effects on R_i, τ_m or capacitance that accounted for its

proposed antagonism.

3.2.2 Action potential firing

We examined Na^+–dependent action potentials evoked by current pulse injection to

determine whether the proposed antagonistic effects of AMBD resulted from alterations

in Na^+ and K^+ channels. Repetitive firing of action potentials was evoked by intracellular

current pulse injection.

Application of AMBD (250 μM) had no effects on action potential firing at 25-40 Hz in

previously untreated (n = 19), bicuculline (20 μM) pre-treated (n = 19) or strychnine (2

μM) pre-treated (n = 19) neurons (cf. Figure 3.2). In addition, there were no significant

Table 3.1 Lack of effects of AMBD on R_i, capacitance and τ_m.

	Control (n = 19)	AMBD (250 μM)
R_i (MΩ)	323 ± 44	222 ± 38
Capacitance (pF)	130 ± 10	120 ± 30
τ_m (ms)	41 ± 6	26 ± 7

	Bicuculline pre-treated (n = 19)	AMBD (250 μM)	Strychnine pre-treated (n = 19)	AMBD (250 μM)
R_i (MΩ)	314 ± 80	294 ± 54	233 ± 35	257 ± 51
Capacitance (pF)	90 ± 10	90 ± 20	110 ± 20	90 ± 40
τ_m (ms)	27 ± 6	25 ± 4	25 ± 7	28 ± 14

Values are mean ± SEM.

effects on action potential amplitude (paired t-test, P < 0.05) or configuration. Half

width of action potentials from previously untreated neurons was 1.0 ± 0.1 ms before

AMBD application and 1.0 ± 0.2 ms after AMBD application (n = 5) (P < 0.05, paired t-

test). These results suggest that the antagonistic effects of AMBD did not likely result

from alteration of voltage-dependent Na^+ or K^+ channels.

3.2.3 Voltage-current relationships

We examined the effects of AMBD (250 μM) on voltage-current relationships to assess

its action on rectifying properties. Furthermore, we examined these before and after

application of bicuculline (20 μM) or strychnine (2 μM) to determine whether AMBD

had actions comparable to these antagonists or whether bicuculline or strychnine altered

AMBD effects.

Figure 3.3 depicts the voltage-current relationships for currents from control (A),

bicuculline pre-treated (B) and strychnine pre-treated (C) neurons and the effects of

AMBD on these currents. After application of AMBD to previously untreated neurons,

the control and drug curves had an intercept of –51 mV (n = 19). The voltage-current

relationship for previously untreated neurons indicated a slight AMBD-mediated

blockade of rectification during large hyperpolarizing pulses. Application of bicuculline

or strychnine alone had no effects on the current intercept. After application of AMBD to
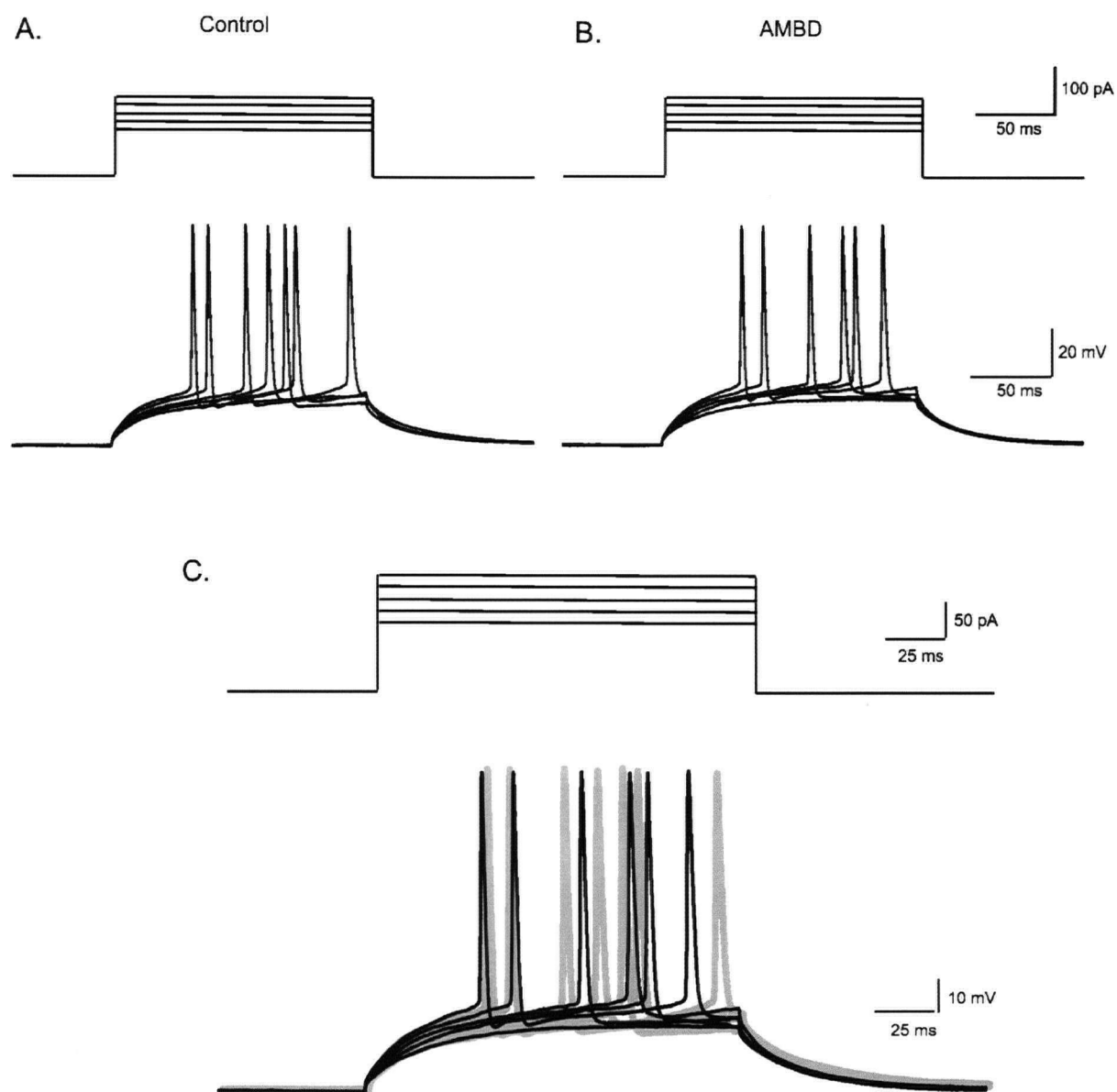
Figure 3.2 AMBD (250 μM) had no effects on action potential firing of a previously untreated neuron. (A) action potential firing of a previously untreated neuron. (B) the same neuron after application of AMBD. (C) control (grey) and AMBD (black) traces were superimposed. Upper traces show injected current pulses and lower traces depict evoked action potentials.

neurons pre-treated with bicuculline, the control and drug curves intercepted at –59 mV

(n = 19). After application of AMBD to neurons pre-treated with strychnine, the

intercept was –58 mV (n = 19). These intercepts were within 6 mVs of E_{Cl} (-53 mV),

suggesting that AMBD had no effects on Cl⁻-mediated currents.

3.2.4 Comparison of effects on baseline currents with bicuculline

Recent studies indicate that gabazine has reversible effects on the baseline GABA-

mediated tonic current in VB neurons (Cope et al., 2005). To determine whether AMBD

(250 μM) acted in a way comparable to gabazine, baseline currents were determined

before and after AMBD application to previously untreated neurons. Alterations in

baseline currents (ΔI) were measured by subtracting baseline current after drug

application from control baseline current adjusted to zero. After application of

bicuculline, ΔI was 46 ± 54 pA. After application of strychnine, ΔI was 38 ± 33 pA. ΔI

after AMBD application was 3 ± 31 pA. Bicuculline, strychnine and AMBD had no

significant effects on baseline current (paired t-tests, P > 0.05).

3.2.5 Summary of effects on membrane properties

In summary, AMBD had no significant effects on R_i, τ_m, or input capacitance. AMBD

did not alter action potential firing frequency, amplitude, configuration or half-width,

hence it likely had no effects on voltage-dependent Na^+ or K^+ channels. Voltage-current

relationships, over a physiological range, showed no significant alteration. The V-I

relationship for previously untreated neurons indicated a slight AMBD-mediated

A. Current (pA)

Voltage (mV)

- ■— Control
- —△—AMBD
- ◆— Strych and Bic

B. Current (pA)

Voltage (mV)

- ■— Control
- ◆—Bicuculline
- —△—AMBD + Bicuculline

C. Current (pA)

Voltage (mV)

- ■— Control
- ◆— Strychnine
- —△—AMBD + Strychnine
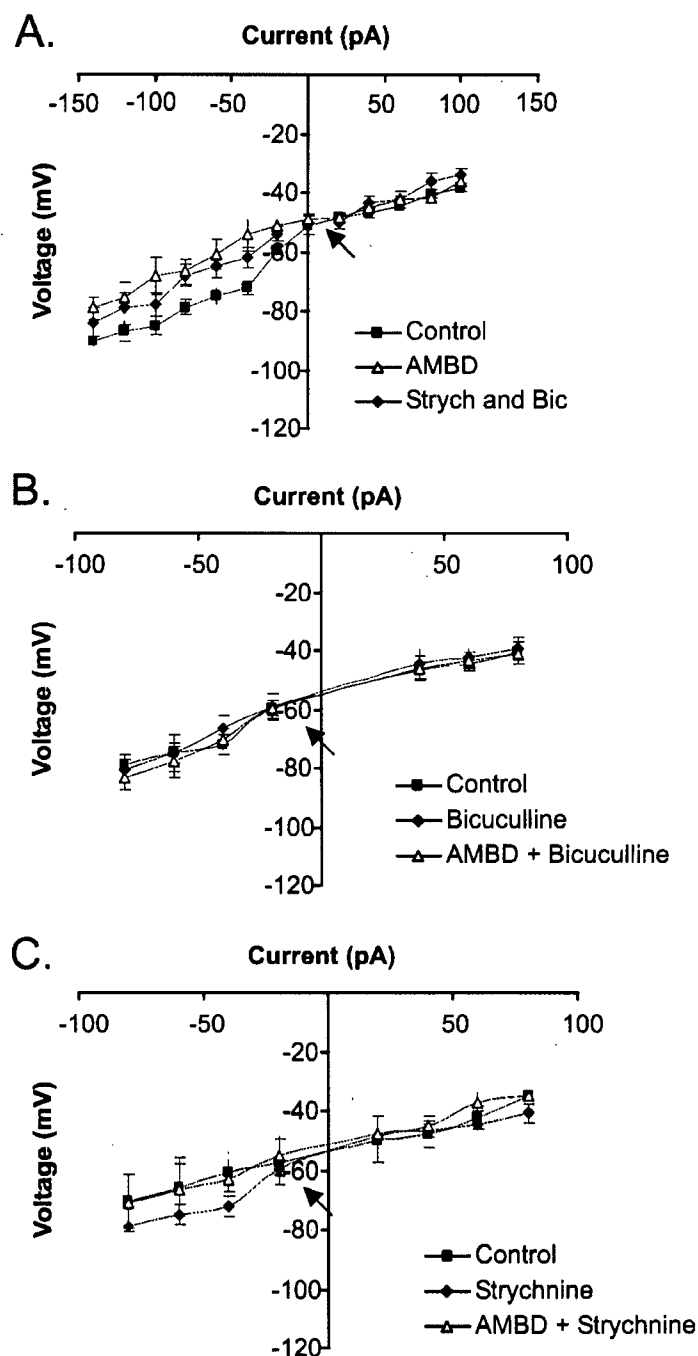
Figure 3.3 Effects of AMBD (250 μM) on voltage-current relationships are shown for currents from control (A), bicuculline (20 μM) pre-treated (B) and strychnine (2 μM) pre-treated (C) neurons. Arrows depict current intercepts obtained from the intersection of control and antagonist curves. Intercepts for control and drug curves were –51 mV (n = 19) for previously untreated, –59 mV (n = 19) for bicuculline pre-treated and –58 mV (n = 19) for strychnine pre-treated neurons.

blockade of rectification during large hyperpolarizing pulses. Although this effect did not alter our results (see below), it may have effects in future current-clamp or *in-vivo* studies. Sulfonamide drugs, including AMBD, have been shown to alter ATP-sensitive K^+ (K_{ATP}) channels, and thereby may alter rectification in this way (Ashcroft and Gribble, 2000). AMBD did not affect the mixed IPSC reversal potential and hence, Cl^- transport processes that maintain $[Cl^-]$ gradients.

3.3 Effects of AMBD on IPSCs

3.3.1 Properties of evoked IPSCs

IPSCs were evoked by electrical stimulation of the ML to determine the effects of AMBD on synaptic inhibition. IPSCs were evoked in 100% of neurons tested (n = 39). The mixed IPSCs (cf. Methods) were further characterized using bicuculline (20 μM) or strychnine (2 μM) to isolate the glycinergic and $GABA_A$ergic components, respectively. The mixed IPSC amplitude was 59 $\pm$ 4.0% $GABA_A$ergic and 41 $\pm$ 4.0% glycinergic (cf. similar values of Ghavanini et al., 2005). Only one of the recorded IPSCs was totally blocked by strychnine, indicating purely glycinergic transmission. 20% of the IPSCs were completely blocked by bicuculline, indicating purely $GABA_A$ergic transmission (n = 5) and 76% (n = 19) had mixed $GABA_A$ergic and glycinergic components.

The average reversal potential of mixed IPSCs was –54 $\pm$ 1.0 mV (n = 19) (Figure 3.5 A). The average reversal potential of isolated glycinergic IPSCs was –52 $\pm$ 1.0 mV and –56 $\pm$ 3.0 mV for isolated $GABA_A$ergic IPSCs. These reversal potentials were not significantly

different from E_{Cl} of -53 mV (One sample t-test, P > 0.05), indicating that the IPSCs

were mediated by Cl⁻.

The latency to IPSCs was also determined. Latency was defined as the time from the

beginning of the stimulus artifact to the onset of the IPSC. The average latency for

mixed IPSCs was 2.0 ± 0.4 ms (n = 19). The average latency for isolated glycinergic and

$GABA_A$ergic IPSCs was 2.0 ± 0.5 ms (n = 19). The latency of the one purely glycinergic

IPSC was 2.3 ms and purely $GABA_A$ergic IPSCs had an average latency of 3.8 ± 1.0 ms

(n = 5). These latencies were not significantly different (paired t-tests, P > 0.05).

3.3.2 Concentration-dependence of IPSC reduction

We anticipated that the proposed antagonistic properties of AMBD would be

concentration-dependent (cf. Mathers, 1993). We determined the concentration-response

relationship for the effects of AMBD on the peak amplitude of mixed IPSCs. Five

concentrations of AMBD were bath applied in a step-wise manner to 7 previously

untreated neurons.

The antagonism of IPSCs by AMBD was concentration-dependent (Repeated measures

ANOVA, P < 0.05). Figure 3.4 depicts the relationship between AMBD concentration

and percentage antagonism of the IPSC. The curve was well-fitted by a single Hill

function with an IC_{50} of 77 μM. The Hill slope was 1.3 ± 0.8, implying that a single

AMBD molecule was required for antagonism (Shirasaki et al, 1991). Based on the
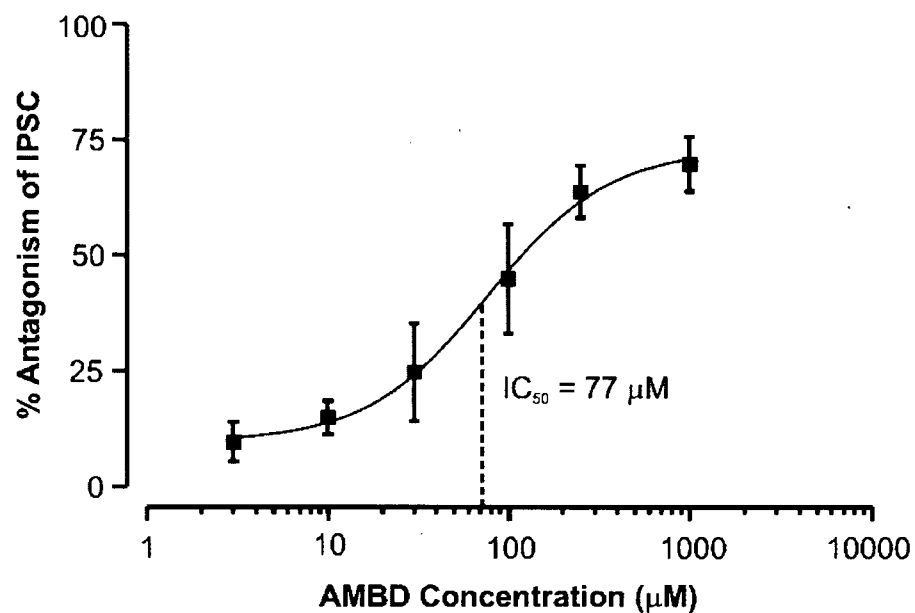
Figure 3.4 Concentration-response relationship for AMBD reduction of IPSCs. AMBD was applied cumulatively in a step-wise manner to neurons held at −80 mV (n = 7 for all points). The dotted line indicates the IC_{50} of 77 μM. Hill slope was 1.3 ± 0.8.

concentration-response curve, the 250 μM AMBD concentration was used for all further experiments.

3.3.3 Reversal potentials of IPSCs

We determined whether AMBD (250 μM) had effects on IPSC reversal potential to determine whether it altered the Cl⁻ gradient. IPSC reversal potential was obtained by changing the holding potential in 10 mV steps between −40 mV and −70 mV. Application of AMBD to mixed IPSCs had no effects on the reversal potential. The average reversal potential of mixed IPSCs after application of AMBD was −53 ± 2.0 mV (n = 19) (Figure 3.5 B). Neither the control nor AMBD reversal potentials differed significantly from E_{Cl} (One sample t-test, P > 0.05). Therefore, AMBD had no effects on the Cl⁻ gradient.

3.3.4 IPSC latency

IPSC latency was measured to determine the effects of AMBD (250 μM) on the time between applied stimulus and IPSC onset. Table 3.2 shows the effects of AMBD on IPSC latency. In summary, AMBD had no significant effects on latency of mixed, isolated or pure IPSCs (paired t-tests, P > 0.05).

3.3.5 Peak amplitudes of mixed IPSCs

The effect of AMBD (250 μM) on mixed IPSCs was determined to identify potential antagonism of the glycinergic and GABA_Aergic components before isolation. Application of AMBD resulted in partial block of mixed IPSCs in every neuron tested (n = 19). The
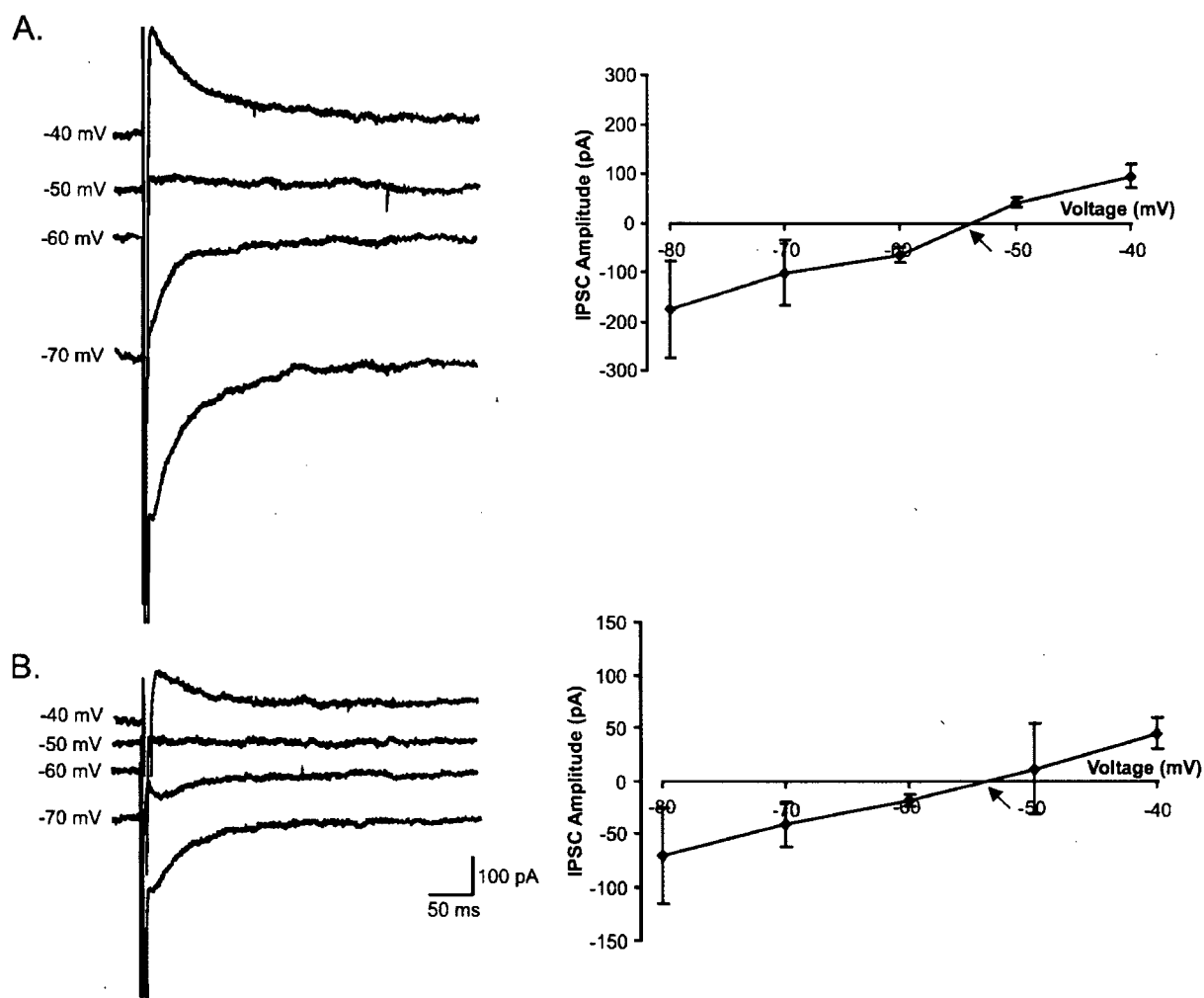
Figure 3.5 AMBD (250 μM) had no effects on mixed IPSC reversal potential. IPSCs (left) and current-voltage relationship (right) of a mixed IPSC before (A) and after (B) AMBD (n = 19). Arrows depict average reversal potential of the mixed IPSC before (-54 ± 1.0 mV) and after AMBD (-53 ± 2.0 mV).

Table 3.2 Effects of AMBD on IPSC latency.

	Mixed (n = 19)	AMBD (250 μM)	
Latency (ms)	2.0 ± 0.4	2.1 ± 0.5	

	Isolated glycinergic (n = 19)	AMBD (250 μM)	Isolated GABA$_A$ergic (n = 19)	AMBD (250 μM)
Latency (ms)	2.0 ± 0.5	2.0 ± 0.7	2.0 ± 0.5	2.2 ± 0.2

	Purely GABA$_A$ergic (n = 5)	AMBD (250 μM)	Purely glycinergic (n = 1)	AMBD (250 μM)
Latency (ms)	3.8 ± 1.0	3.5 ± 0.7	2.3	3.1

Values are mean ± SEM.

average reduction in peak amplitude of the mixed IPSC was 67 ± 5.0%. Figure 3.6

depicts the effects of AMBD on a representative mixed IPSC.

3.3.6 Time course of antagonism and recovery

We determined the time course of action and recovery for AMBD (250 µM) antagonism.

Percentage inhibition of the peak amplitude of a mixed IPSC was measured every minute

during the application of AMBD and every 15 minutes after terminating application.

Peak amplitude reduction began within 2 to 4 minutes after initiating application and

showed no further reduction after 10 minutes (n = 5). Full recovery was not recorded

despite stable recording for periods up to 1.5 hours. Partial recovery was observed in 6

neurons. Partial recovery from AMBD began within 30 to 45 minutes and was complete

within 60 minutes (n = 6) (Figure 3.7). Past studies using an identical bath perfusion

technique showed that complete recovery from bicuculline required 30 minutes or less.

Hence, the rate-limiting step in AMBD recovery was not perfusion, but likely, tissue

uptake and binding characteristics.

3.3.7 Pharmacologically isolated IPSCs

The effects of AMBD on isolated glycinergic and $GABA_A$ergic IPSCs were examined to

determine whether the observed mixed IPSC antagonism resulted from reduction of one

or both components. Glycinergic and $GABA_A$ergic components were isolated from the

mixed IPSC using bicuculline (20 µM) and strychnine (2 µM), respectively. Application

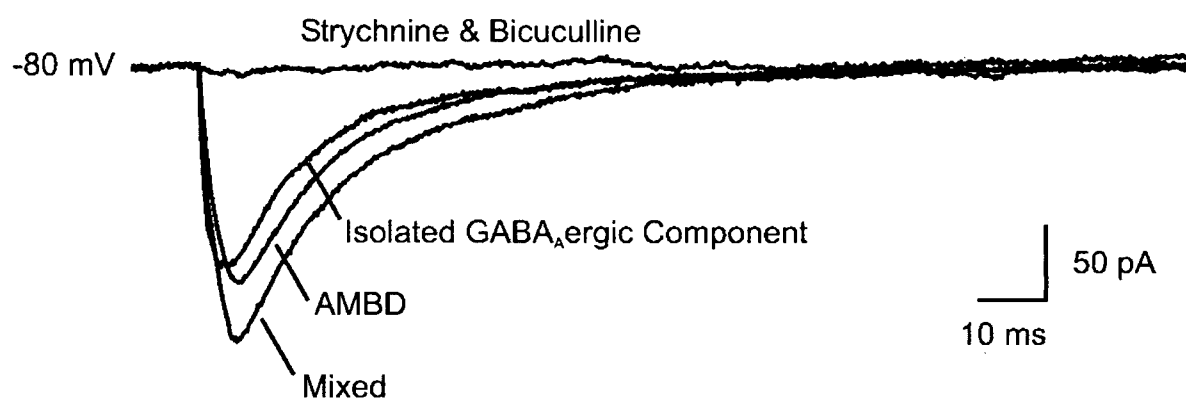of AMBD (250 µM) to 19 neurons with the isolated glycinergic component resulted in

Figure 3.6 AMBD (250 µM) decreased the peak amplitude of a representative mixed IPSC by 24 pA (25%).
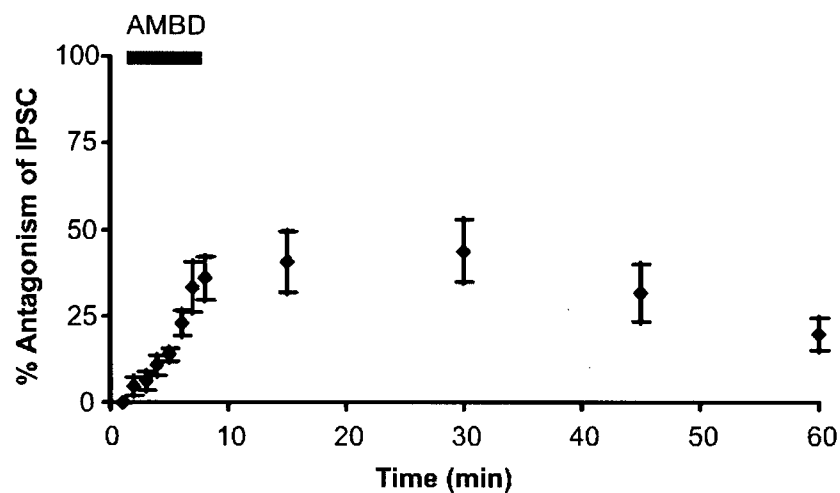
Figure 3.7 Time course for AMBD (250 µM) reduction of the mixed IPSC and recovery. Percentage antagonism of peak amplitude recorded every minute for 8 minutes during AMBD application (n = 5) and every 15 minutes during AMBD washout (n = 6).

reduction of this current in 12 neurons (63%) and no effect in 7 neurons (37%). AMBD reduced the peak amplitude of the isolated glycinergic IPSC by an average of 41 ± 11% (n = 19). AMBD reduced the isolated GABA$_A$ergic IPSC in 79% (n = 15), and had no effect in 21% (n = 4). AMBD reduced the isolated GABA$_A$ergic IPSC peak amplitudes by an average of 70 ± 18.0% (n = 19). Figure 3.8 depicts the pharmacological isolation of glycinergic and GABA$_A$ergic components from a mixed IPSC and the effects of AMBD on these components. Our observations indicated that mixed IPSC antagonism resulted from AMBD actions on both the isolated glycinergic and the GABA$_A$ergic components. The total antagonism approximated the amount of reduction observed in mixed IPSCs.

3.3.8 Comparison of antagonism with strychnine

We determined whether AMBD antagonized the glycine receptor like strychnine. To assess whether AMBD reduced the mixed and isolated IPSCs in a manner similar to strychnine, we compared average percentage inhibitions of peak IPSC amplitude induced by AMBD (250 μM), strychnine (2 μM) and bicuculline (20 μM). The mixed IPSC peak amplitude was reduced by AMBD (67 ± 5%), bicuculline (59 ± 4%) and strychnine (41 ± 4%) (n = 19). Percentage inhibitions of the mixed IPSC by AMBD and bicuculline were not significantly different (paired t-test, P > 0.05) but percentage inhibitions by AMBD and strychnine were significantly different (paired t- test, P < 0.05). AMBD produced less antagonism of the isolated glycinergic IPSC (41 ± 11%) than strychnine (96 ± 1%) (n = 19) (paired t-test, P < 0.05). The isolated GABA$_A$ergic IPSC was reduced by AMBD

A.

Bicuculline & Strychnine

-80 mV

Isolated Glycinergic Component

Mixed

B.

-80 mV

AMBD

Isolated Glycinergic Component

C.

-80 mV

AMBD

25 pA

10 ms

Isolated GABA$_A$ergic Component
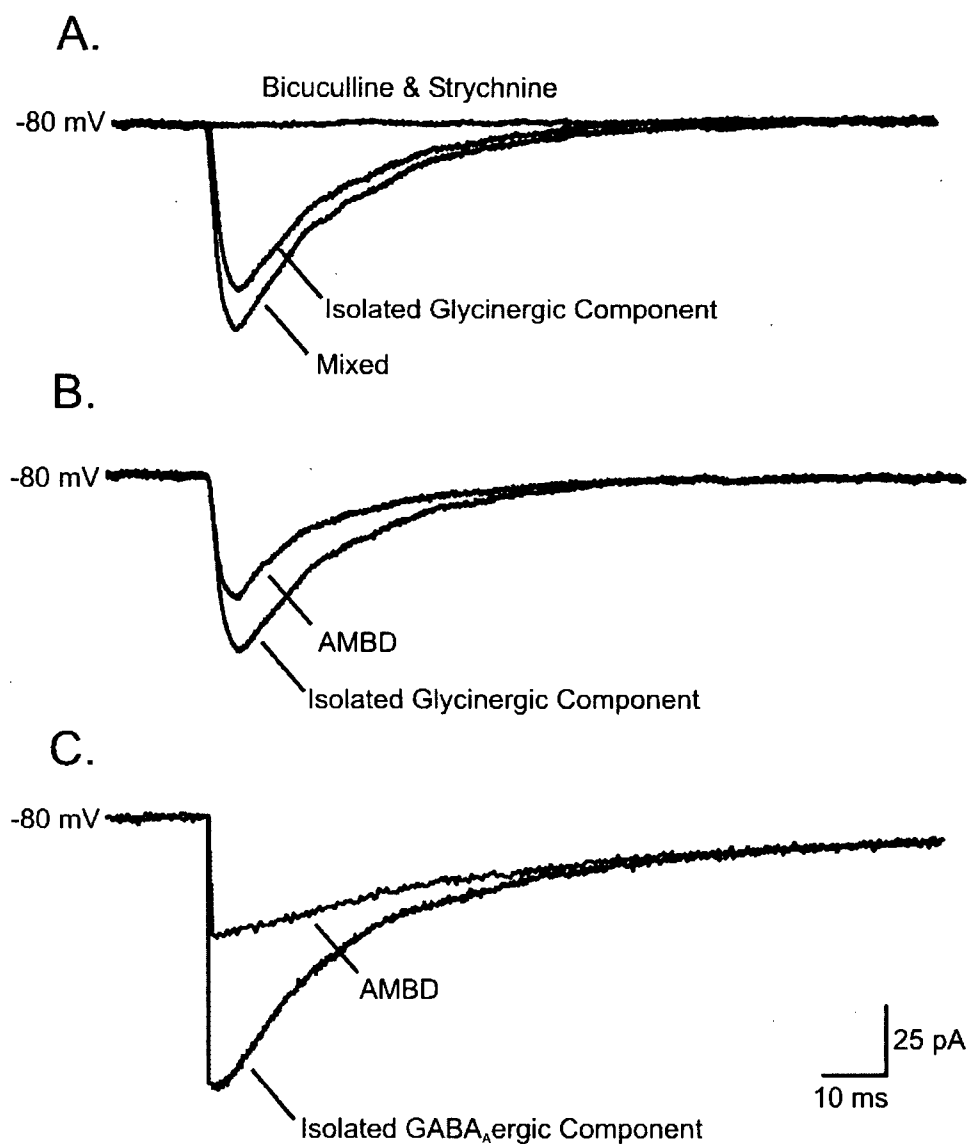
Figure 3.8 AMBD (250 μM) reduced the peak amplitude of isolated glycinergic and GABA$_A$ergic IPSCs in 2 neurons (A, B, C). (A) bicuculline (20 μM) and strychnine (2 μM) revealed distinct glycinergic and GABA$_A$ergic components. (B) AMBD reduced the isolated glycinergic component. (C) AMBD reduced the isolated GABA$_A$ergic component.

(70 ± 18%) and bicuculline (98 ± 1%) (n = 19). Percentage inhibitions of the isolated

GABA$_A$ergic IPSC by AMBD were significantly less than percentage inhibitions by

bicuculline (paired t-test, P < 0.05). AMBD reduced the mixed IPSC to a greater extent

than strychnine and decreased the glycinergic and GABA$_A$ergic IPSCs after their

pharmacological isolations (Figure 3.9). In summary, AMBD did not antagonize the

glycine receptor to the same extent as strychnine, and additionally exhibited properties of

a GABA$_A$ antagonist.

3.3.9 Purely glycinergic and GABA$_A$ergic IPSCs

The effects of AMBD (250 μM) were also examined on one purely glycinergic and 5

purely GABA$_A$ergic IPSCs. In one neuron, AMBD reduced the peak amplitude of the

glycinergic IPSC by 81%. Strychnine eliminated the purely glycinergic IPSC.

Interestingly, AMBD had no effects on 4 GABA$_A$ergic IPSCs and partially antagonized 1

GABA$_A$ergic IPSC by 17% (Figure 3.10). AMBD reduced the purely glycinergic IPSC

in one neuron but had no effect on the majority of purely GABA$_A$ergic IPSCs, suggesting

potential specificity for the glycine receptor.

3.3.10 Rise time and charge transfer

Before AMBD antagonism, strychnine (2 μM) and bicuculline (20 μM) had no

significant effects on the rise time of mixed, pure and isolated glycinergic and

GABA$_A$ergic IPSCs (paired t-tests, P > 0.05). Hence, we were able to attribute any

potential effects exclusively to AMBD.
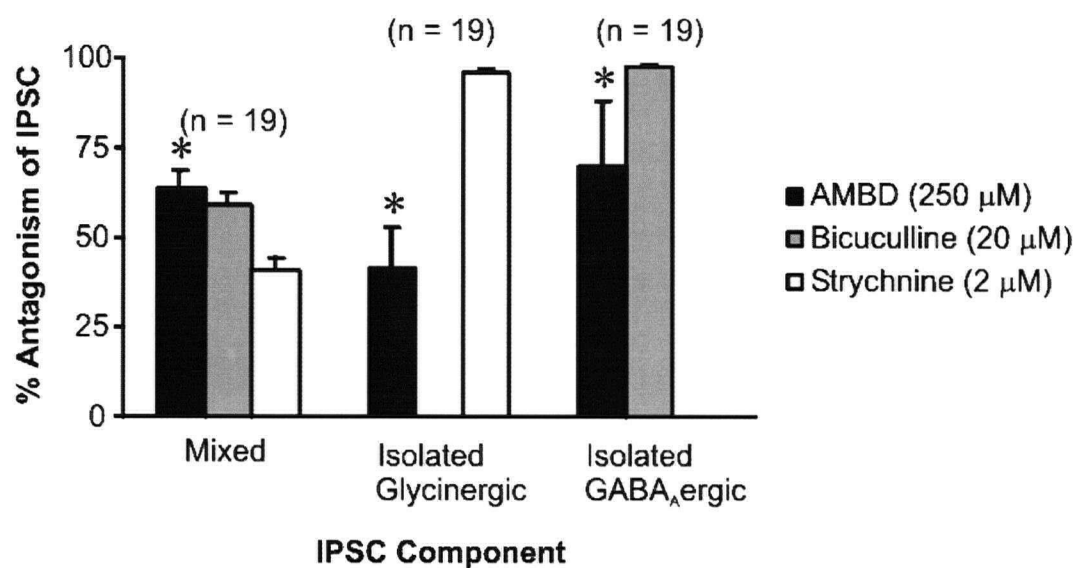
Figure 3.9 Comparison of the effects of AMBD with strychnine and bicuculline on mixed and isolated IPSCs. Values are mean ± SEM. Asterisks indicate that percentage antagonisms of the mixed and isolated glycinergic IPSCs by AMBD and strychnine, and of the isolated GABA$_A$ergic IPSCs by AMBD and bicuculline, were statistically different from each other (P < 0.05, paired t-tests).

A.

Strychnine & Bicuculline

-80 mV

AMBD

Purely Glycinergic

B.

Bicuculline

-80 mV

Purely GABA$_A$ergic, AMBD

50 pA

10 ms
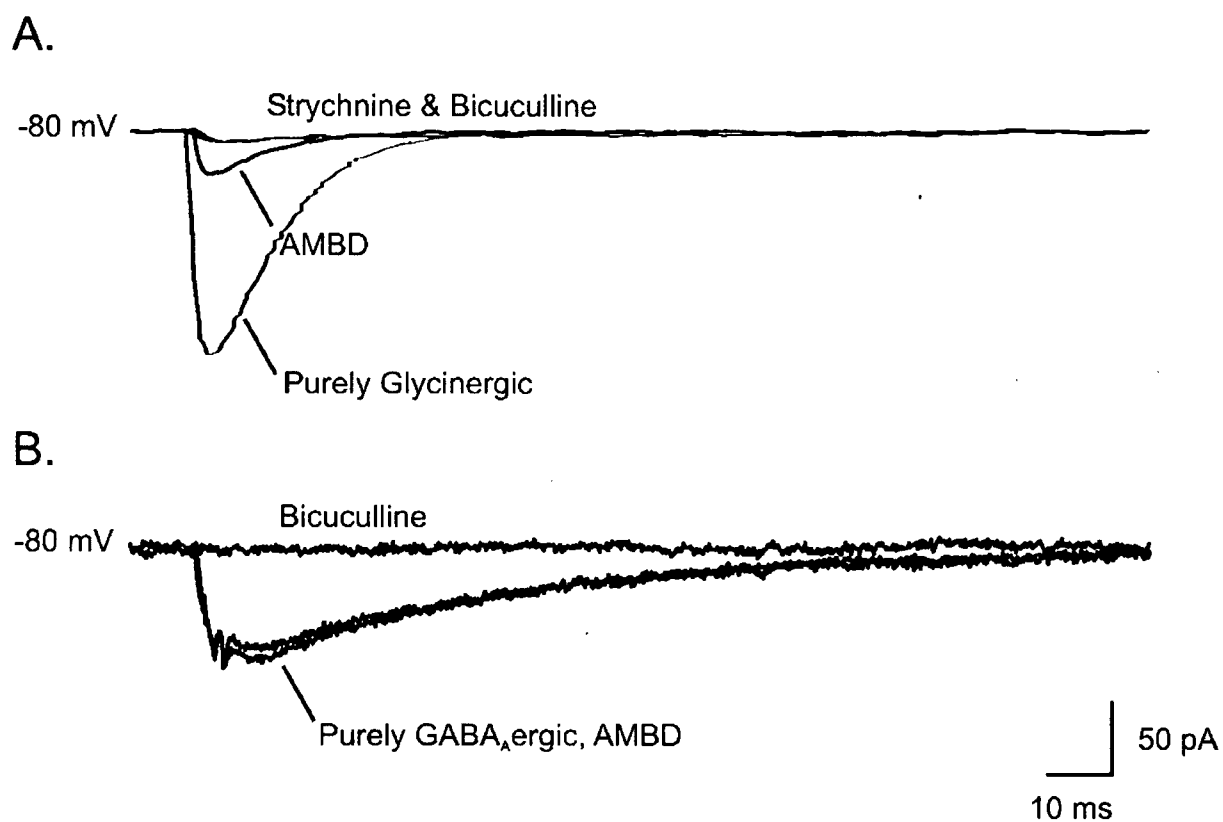
Figure 3.10 AMBD (250 µM) exhibited selectivity in antagonism. AMBD reduced a purely glycinergic IPSC (A) but had no effects on purely GABA$_A$ergic IPSCs (B).

AMBD had no significant effects on the rise time of mixed, pure, and isolated glycinergic and GABA$_A$ergic IPSCs (paired t-tests, P > 0.05). Table 3.3 summarizes the rise times of IPSCs before and after AMBD. Rise time was not associated with IPSC antagonism by AMBD.

We calculated percentage inhibition of charge transfer for mixed, pure and isolated glycinergic and GABA$_A$ergic IPSCs. AMBD (250 μM) had no significant effects on charge transfer of mixed IPSCs, with an average reduction of 43 ± 11% (n = 19) (P > 0.05, paired t-test). AMBD also had no significant effects on charge transfer of isolated GABA$_A$ergic IPSCs, with an average reduction of 59 ± 17% (n = 19) (P > 0.05, paired t-test). AMBD had no significant effects on the isolated glycinergic components charge transfer, with an average reduction of 49 ± 8 % (n = 19) (P > 0.05, paired t-test). AMBD (250 μM) reduced charge transfer of the purely glycinergic IPSC by 85% (n = 1). Lastly, AMBD had no significant effects on the charge transfer of purely GABA$_A$ergic IPSCs (n = 4), with an average reduction of 2 ± 2% (Table 3.3) (P > 0.05, paired t-test). In contrast to the AMBD reduction in IPSC peak amplitude, measurements of charge transfer were associated with large variations in SEM, contributing to an inability to demonstrate significance.

Table 3.3 Summary of the effects of AMBD on rise time and charge transfer of mixed and pure IPSCs, and isolated components.

	Control (n = 19)	AMBD (250 μM)
Rise Time (ms)	1.0 ± 0.5	1.0 ± 0.5
Area (pC)	-6.7 ± 1.7	-4.4 ± 2.2

	Isolated glycinergic (n = 19)	AMBD (250 μM)	Isolated GABA$_A$ergic (n = 19)	AMBD (250 μM)
Rise Time (ms)	1.0 ± 0.5	2.0 ± 1.0	1.0 ± 0.5	1.0 ± 1.0
Area (pC)	-0.7 ± 0.3	-0.9 ± 0.5	-5.9 ± 2.1	-4.7 ± 4.0

	Purely GABA$_A$ergic (n = 4)	AMBD (250 μM)	Purely glycinergic (n = 1)	AMBD (250 μM)
Rise Time (ms)	1.0 ± 0.5	2.0 ± 1.0	1.0	1.0
Area (pC)	-0.4 ± 0.2	-0.5 ± 1.1	-5.1	-0.8

Values are mean ± SEM.

3.4 Effects of AMBD on IPSC decay

3.4.1 Fast, intermediate and slow IPSC decay

Previous studies suggested that mixed IPSCs in the VB nuclei had slow and fast decay

time constants attributable to glycine receptor activation, whereas $GABA_A$ergic IPSCs

had intermediate decay time constants (Ghavanini et al., 2006). We determined whether

AMBD had effects on the decay of mixed IPSCs or isolated components and whether

these effects were alike to the observed IPSC reduction. IPSC decay phases were fitted

with exponential terms to determine the time constants. The decay time constants

differed slightly from Ghavanini et al. (2006), presumably because of recordings from a

differing neuronal sample.

3.4.2 Intermediate and slow IPSC components

The mixed IPSCs decayed with a biexponential time course and were separatable into

two groups based on differential strychnine- and bicuculline-sensitivity: (1) IPSCs with

bicuculline-sensitive intermediate (21 ± 0.5 ms) and strychnine-sensitive fast (8 ± 1.0 ms)

time constants (n = 14), and (2) IPSCs with bicuculline-sensitive intermediate (19 ± 2.0

ms) and strychnine-sensitive slow (101 ± 12.0 ms) time constants (n = 10). The fast,

intermediate and slow time constants were significantly different from each other (One

way ANOVA, $P < 0.05$).

Application of AMBD (250 μM) to group (1) neurons eliminated the intermediate IPSC

component. The remaining component had a time constant of 6 ± 1.0 ms, which was not

significantly different from the control fast component (paired *t*-test, $P > 0.05$).

Application of AMBD to group (2) neurons eliminated the slow IPSC component, leaving a current with a time constant of 13 ± 3.0 ms, which was not significantly different from the control intermediate component (paired t-test, $P > 0.05$) (Figure 3.11, Table 3.4). Histograms of decay time constants are shown in Figure 3.12. AMBD abolished the intermediate and slow components in mixed IPSCs, and had no effects on the fast components.

3.4.3 Pharmacologically isolated decays

The observed AMBD-mediated reduction in isolated glycinergic IPSC amplitude (see above) was not associated with alterations in decay. Isolation of the glycinergic component from the mixed IPSC containing fast and intermediate components revealed a monoexponential decay time constant of 8 ± 1.0 ms (n = 4). The time constant was not significantly different from the mixed IPSC fast constant (paired t-test, $P > 0.05$). The glycinergic component isolated from a mixed IPSC containing intermediate and slow time constants had a single decay time constant of 83 ms (n = 1).

The observed AMBD-mediated reduction in isolated $GABA_A$ergic IPSC amplitude (see above) was also not associated with alterations in decay. Isolation of the $GABA_A$ergic component from mixed IPSCs with fast and intermediate components revealed a single decay time constant of 15 ± 3.0 ms (n = 8). The time constant was not significantly different from the mixed IPSC intermediate constant (paired t-test, $P > 0.05$). The
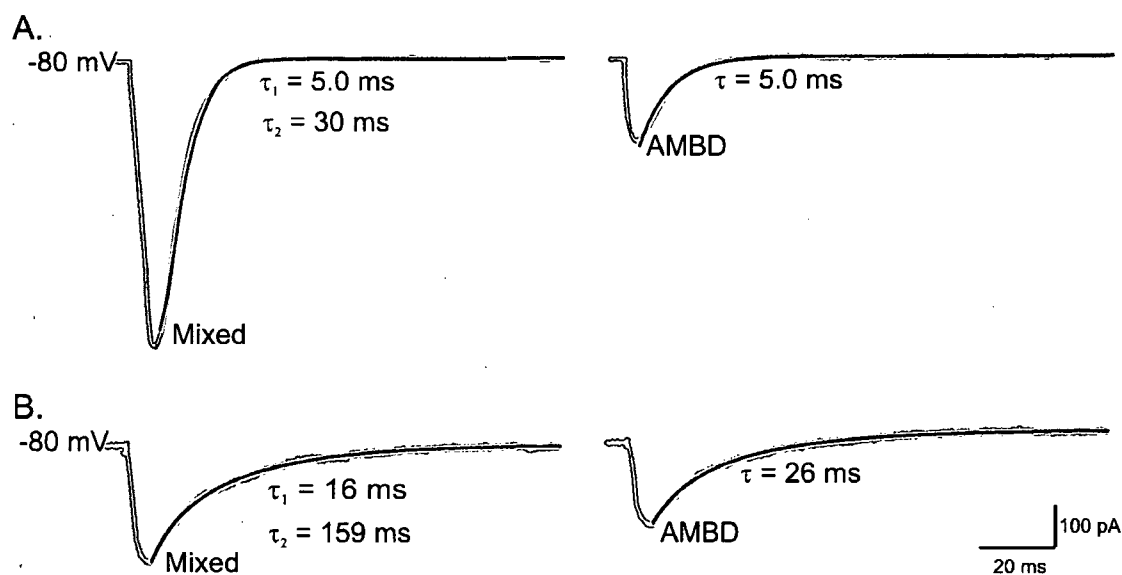
Figure 3.11 Effects of AMBD (250 µM) on the decay time constants of mixed IPSCs with fast and intermediate time constants (A) and mixed IPSCs with intermediate and slow time constants (B). IPSCs were fitted with mono- or bi-exponentials (black).

Table 3.4 Effects of AMBD on decay parameters of mixed IPSCs.

Mixed IPSCs with fast and intermediate components

Component	Parameter	Control (n = 14)	AMBD (250 μM)
Fast	Time constant (ms)	8 ± 1.0	6 ± 1.0
	Amplitude (pA)	-375 ± 124	-215 ± 101 *
Intermediate	Time constant (ms)	21 ± 0.5	0
	Amplitude (pA)	-123 ± 43	0

Mixed IPSCs with intermediate and slow components

Component	Parameter	Control (n = 10)	AMBD (250 μM)
Intermediate	Time constant (ms)	19 ± 2.0	13 ± 3.0
	Amplitude (pA)	-205 ± 96	-136 ± 22 *
Slow	Time constant (ms)	101 ± 13	0
	Amplitude (pA)	-22 ± 4	0

Values are mean ± SEM. * $P < 0.05$ (paired *t*-test).
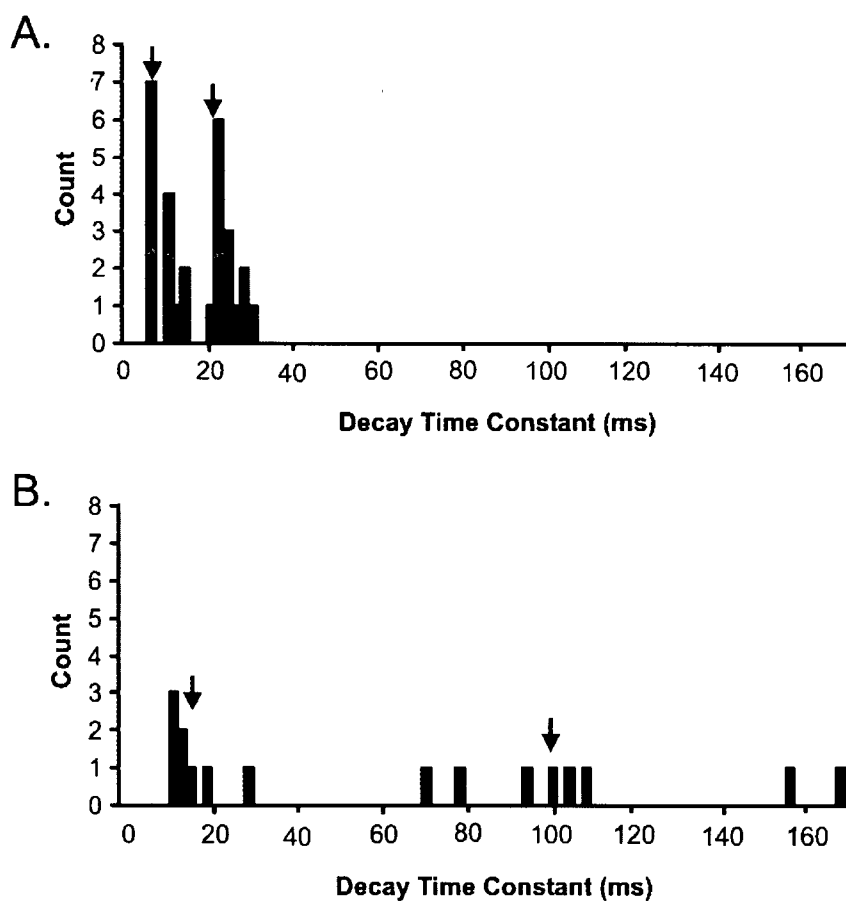
Figure 3.12 Histograms of the decay time constants of mixed IPSCs. Mixed IPSCs that decayed with a biexponential time course were separated into 2 groups. (A) the first group had a bicuculline-sensitive intermediate (21 ± 0.5 ms) and a strychnine-sensitive fast (8 ± 1.0 ms) component (n = 14), arrows. (B) the second group had a bicuculline-sensitive intermediate (19 ± 2.0 ms) and a strychnine-sensitive slow (101 ± 12.0 ms) component (n = 10), arrows.

GABA$_A$ergic component from mixed IPSCs with intermediate and slow time constants had an intermediate decay time constant of 19 ± 3.0 ms (n = 7). The time constant was not significantly different from the mixed IPSC intermediate component (paired t-test, P > 0.05).

These results are consistent with previously published decay time constants for isolated glycinergic and GABA$_A$ergic IPSCs (Ghavanini et al., 2006). As summarized in Table 3.5, AMBD (250 μM) had no significant effects on the isolated glycinergic or GABA$_A$ergic IPSC decay time constants (paired t-test, P > 0.05) (Figure 3.13).

3.4.4 Purely glycinergic and GABA$_A$ergic decays

The decay time constants of purely glycinergic and GABA$_A$ergic IPSCs were determined to establish whether the observed IPSC antagonism was associated with alterations in decay. The decay of the purely glycinergic IPSC had a single decay time constant of 6.0 ms (n = 1). The decay of the purely GABA$_A$ergic IPSCs had a single intermediate decay time constant of 19 ± 1.0 ms (n = 4). AMBD (250 μM) had no effects on decay time constants of purely glycinergic and GABA$_A$ergic IPSCs. The respective time constants were 6.0 ms (n = 1) and 17 ± 1.0 ms (n = 4) (paired t-test, P > 0.05 for GABA$_A$ergic) (Figure 3.14, Table 3.6). Glycinergic IPSC antagonism by AMBD and its failure to antagonize GABA$_A$ergic IPSCs were not associated with changes in decay.
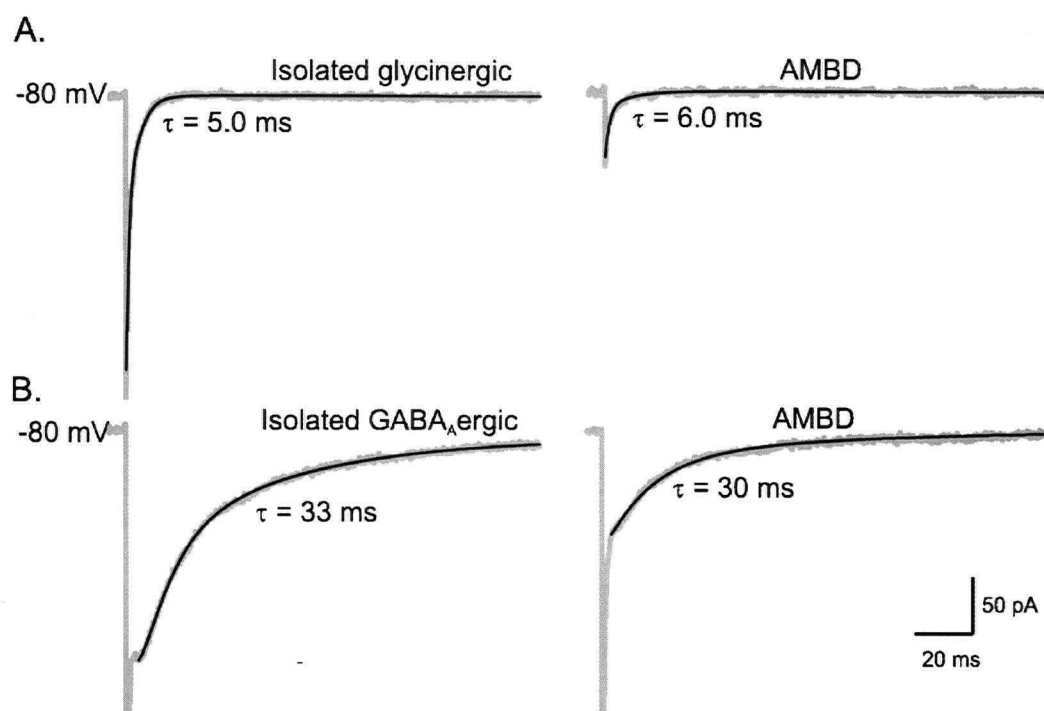
Figure 3.13 Lack of effect of AMBD (250 μM) on the decay time constants of isolated glycinergic (A) or GABA$_A$ergic (B) IPSCs. IPSCs were fitted with single exponentials (black).

Table 3.5 Effects of AMBD on decay time constants and amplitudes of exponentially fitted isolated glycinergic and GABA$_A$ergic IPSCs.

Isolated from IPSCs with fast and intermediate components

Parameter	Glycinergic (n = 4)	AMBD (250 μM) (n = 4)	GABA$_A$ergic (n = 8)	AMBD (250 μM) (n = 1)
Time constant (ms)	8 ± 1.0	9 ± 1.0	15 ± 3.0	19
Amplitude (pA)	-317 ± 90	-288 ± 85	-164 ± 95	-520

Isolated from IPSCs with intermediate and slow components

Parameter	Glycinergic (n = 1)	AMBD (250 μM) (n = 1)	GABA$_A$ergic (n = 7)	AMBD (250 μM) (n = 1)
Time constant (ms)	83	15	19 ± 3.0	30
Amplitude (pA)	-58	-9	-121 ± 47	-44

Values are mean ± SEM.
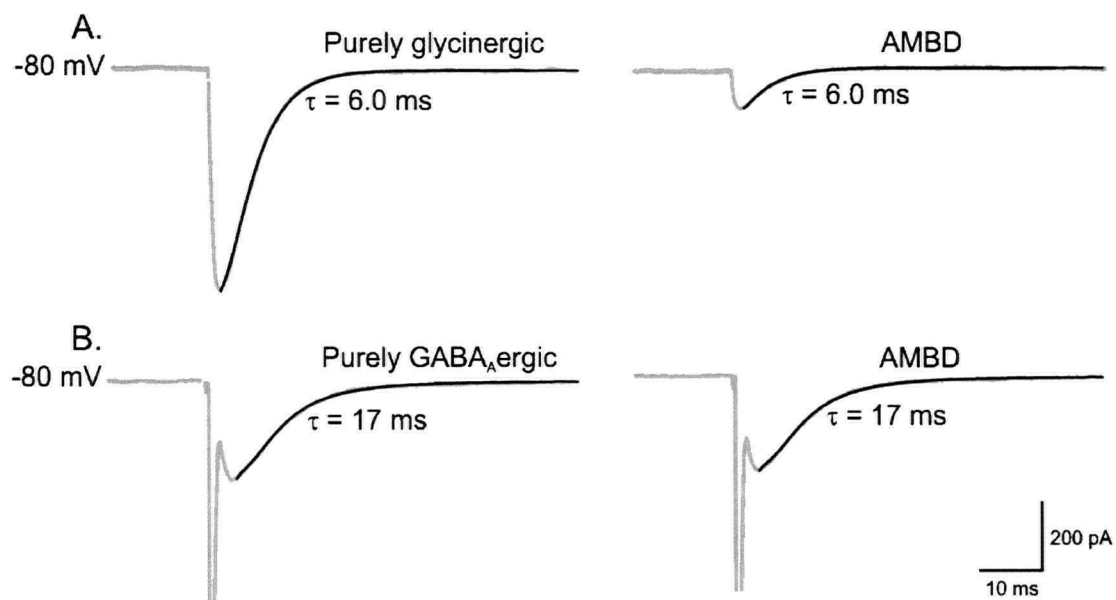
Figure 3.14 AMBD (250 μM) effects on the decay time constants of purely glycinergic (A) or GABA$_A$ergic (B) IPSCs. The IPSCs were fitted with single exponentials (black).

Table 3.6 Effects of AMBD on decay time constants and amplitudes of exponentially fitted glycinergic and GABA$_A$ergic IPSCs.

Parameter	Purely GABA$_A$ergic (n = 4)	AMBD (250 µM)	Purely glycinergic (n = 1)	AMBD (250 µM)
Time constant (ms)	19 ± 1.0	17 ± 1.0	6	6
Amplitude (pA)	-26 ± 9	-25 ± 11	-1030	-124

Values are mean ± SEM.

3.5 Spontaneous IPSCs

We determined the effects of AMBD on sIPSCs to assess possible presynaptic actions.

Without AMBD, we recorded an average sIPSC frequency of 1.0 ± 0.2 Hz (n = 5). The

average amplitude of sIPSCs was -19 ± 2 pA (n = 5). The average rise time of sIPSCs

was 1.0 ± 0.3 ms (n = 5). There was no correlation between the amplitude, rise time and

decay time constants of the detected events ($R^2 < 0.05$) (Figure 3.15). Hence, the

detected events were sIPSCs and not random noise.

AMBD (250 µM) significantly decreased the frequency of sIPSCs to 0.2 ± 0.03 Hz (P <

0.05, paired t-test) (Figure 3.16). After AMBD application, the amplitude of sIPSCs was

-19 ± 3 pA, which was not different from control (P > 0.05, paired t-test). The rise time

of sIPSCs after AMBD application was 1.0 ± 0.4 ms, which was not different from

control (P > 0.05, paired t-test). Table 3.7 summarizes the effects of AMBD on sIPSCs.
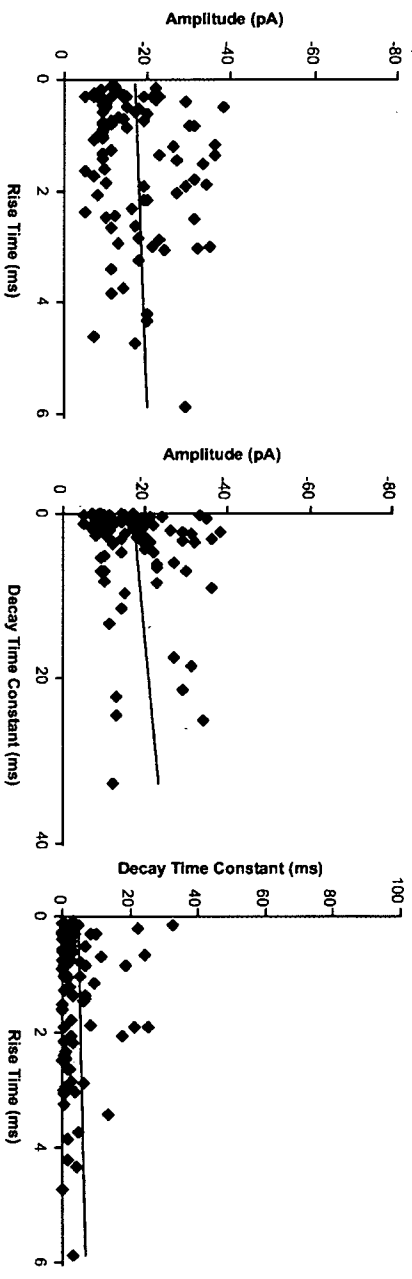
Figure 3.15 Lack of correlation between amplitude, rise time and decay time constants of spontaneous IPSCs ($R^2 < 0.05$).

57

Figure 3.16 AMBD decreased the frequency but not the amplitude of sIPSCs. Arrows indicate visually accepted sIPSCs.

Table 3.7 Summary of AMBD effects on spontaneous IPSCs.

	Control (n = 5)	AMBD (250 μM)
Frequency (Hz)	1.0 ± 0.2	0.2 ± 0.03 *
Amplitude (pA)	19 ± 2	19 ± 3
Rise time (ms)	1.0 ± 0.3	1.0 ± 0.4

Values are mean ± SEM. * P <0.05, paired *t*-test.

Chapter IV. Discussion

4.1 Summary of the results

This thesis studied the effects of a potential glycine receptor antagonist, AMBD, on

neurons in the VB nuclei of the thalamus. The aim was to assess the ability of AMBD to

selectively antagonize IPSCs and sIPSCs in VB neurons. The hypothesis was that

AMBD interacts with synaptic glycine receptors and not $GABA_A$ receptors, to

specifically suppress the inhibitory effects of glycine-like amino acids.

AMBD significantly reduced the peak amplitude of electrically stimulated mixed IPSCs,

pharmacologically isolated IPSCs, and purely glycinergic IPSCs. The reduction of peak

amplitude of mixed IPSCs by AMBD was concentration-dependent, with an IC_{50} of 77

μM and a Hill slope of ~ 1.3. Like strychnine, AMBD had no effects on four purely

$GABA_A$ergic IPSCs, or their time constants.

AMBD did not antagonize IPSCs in a manner identical to strychnine. AMBD abolished

the intermediate and slow components of mixed glycinergic and $GABA_A$ergic IPSCs,

whereas strychnine eliminated the fast, as well as the slow, components of mixed IPSCs.

AMBD had no effects on the decay time constants of pharmacologically isolated IPSCs.
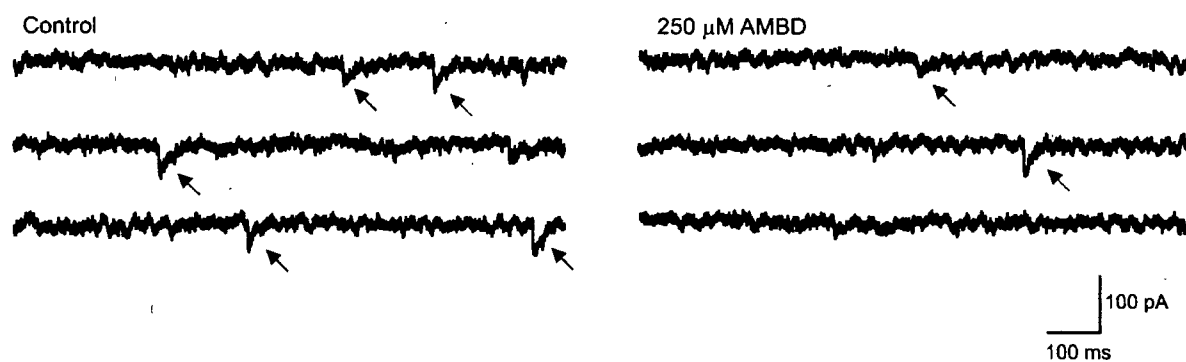
AMBD decreased the apparent frequency but not the amplitude of spontaneous IPSCs

(sIPSCs). AMBD had little or no effects on the passive and active membrane properties

that could account for the observed antagonism. It therefore remains to succinctly

discuss the findings that are most relevant to an assessment of AMBD as a selective

antagonist of receptors for amino acids.

4.2 Postsynaptic receptor antagonism by AMBD

4.2.1 Mixed IPSCs

We have shown for the first time, that AMBD significantly reduced the peak amplitude by ~ 67% of mixed glycinergic and GABA$_A$ergic IPSCs in 19 thalamocortical neurons. These studies also confirmed that glycinergic and GABA$_A$ergic receptors mediate the mixed IPSCs evoked by electrical stimulation of the medial lemniscus (ML) (cf. Ghavanini et al. 2005). The mixed IPSC likely results from release of several glycine-like amino acids and GABA from co-transmitting glycinergic and GABA$_A$ergic pathways (cf. Ghavanini et al., 2005). Although purely glycinergic and GABA$_A$ergic IPSCs were observed in several neurons, it was necessary to isolate the glycinergic and GABA$_A$ergic components from the mixed IPSCs with strychnine or bicuculline for a detailed analysis of AMBD actions.

4.2.2 Isolated and purely glycinergic currents

We showed that bicuculline antagonized the GABA$_A$ergic component of the mixed IPSC, evident as a decrease in peak amplitude. Concomitant application of strychnine abolished the remaining component. AMBD antagonized the peak amplitude of the latter, glycinergic component by ~ 41% in 19 neurons. AMBD also reduced the peak amplitude of purely glycinergic IPSCs by 81% in one neuron. By comparison, strychnine produced ~ 96% antagonism of the glycinergic component in the same 19 neurons, and eliminated the purely glycinergic IPSCs in one neuron. Although less potent than strychnine, AMBD was an effective antagonist of glycinergic inhibition in VB thalamus.

4.2.3 Isolated and purely GABA$_A$ergic currents

Unexpectedly, the actions of AMBD were not entirely specific for glycinergic receptors, and blocked GABA$_A$ergic IPSCs after isolation with strychnine. AMBD reduced the peak amplitude of isolated GABA$_A$ergic IPSCs by ~ 70% in 19 neurons. AMBD did not alter purely GABA$_A$ergic IPSCs in four out of five neurons. The purely GABA$_A$ergic IPSCs altered by AMBD in one neuron may have been mixed, with a small glycinergic component, therefore these were excluded from further analysis (cf. Results).

An explanation for the additional antagonism at the GABA$_A$ receptor is that, the GABA$_A$ergic current associated with the mixed IPSC may differ in pharmacological sensitivity from purely GABA$_A$ergic IPSCs. The specificity of released glycine-like amino acids for the synaptic glycine receptor may not be uniformly absolute, since β– alanine can additionally affect the GABA$_A$ receptor (cf. Wu et al., 1993). Thus, AMBD antagonism may critically depend on the type of agonist interacting with the GABA$_A$ receptor or equivocally, access of antagonists to the mixed and isolated receptor sites.

This explanation implies that purely GABA$_A$ergic currents may be mediated by a different GABA$_A$ receptor than the isolated GABA$_A$ergic currents. AMBD could block a new postsynaptic receptor with an unknown subunit composition or act at a distinct binding site on the GABA$_A$ receptor that is sensitive to AMBD (cf. Kuhse et al., 1990). The mixed IPSC presumably results from glycine, taurine, and β–alanine, with unknown release-stoichiometry, as well as GABA. Although the exact stoichiometry is unknown,

specificity of AMBD for the β–amino acids, and less for glycine, could explain the reduced potency of AMBD on mixed IPSCs, in comparison to strychnine. Numerous studies in the CNS have suggested the existence of a β–amino acid receptor that is relatively insensitive to glycine but activated by taurine and β–alanine (reviewed by Huxtable, 1989).

4.2.4 The potential β–amino acid receptor

Studies on concentration-response relationships for glycine and the β–amino acids have revealed discrepancies in medullary neurons that provide evidence for a distinct β–amino acid receptor. The Hill slopes for the agonist actions of glycine and β–amino acids were not similar in the medulla (Gatti et al., 1985), suggesting that their effects were mediated by different receptors or by different binding sites on the same receptor. In the VB nuclei, the concentration-response curves for the agonist actions of β–alanine, glycine and taurine have different slopes (cf. Ghavanini et al., 2005). Furthermore, the latter studies showed that co-application of strychnine and bicuculline did not completely block the effects of β-alanine, although the reversal potential for its action indicated Cl⁻ mediation. These results suggest that β–amino acid receptors or uncharacterized sites on the glycine or $GABA_A$ receptor mediate the effects of β–amino acids.

The existence of a β–amino acid receptor may require evidence for high-affinity, Na^+-independent binding of β–amino acids, in contrast to membrane transporters. The specific binding to receptors is Na^+-independent, whereas binding of agonists to transporters is Na^+-dependent (Huxtable, 1989). Although AMBD-sensitive, Na^+-

independent binding of taurine to brain synaptosomes has been reported for cerebral cortex (Kontro and Oja, 1983; Kontro et al., 1984; Kontro and Oja, 1987), these results are considered inconclusive because of the use of a homogenized tissue preparation (cf. Huxtable, 1989).

4.3 Effects of AMBD on decay of mixed IPSCs

4.3.1 Slow decay time constant

An outstanding effect of AMBD was the elimination of the slow component of mixed IPSCs comprised of slow and intermediate components, in all 10 neurons. The IPSC decay time constant is similar to extrasynaptic channel burst duration during glycine and β–amino acid application in the VB nuclei (Ghavanini et al., 2006). The lifetimes of channel bursts (cf. Beato et al., 2002) likely mediate the decay time constant of IPSCs. The average lifetimes of short- and long-duration bursts were similar to the decay time constants of fast and slow IPSCs, respectively (Ghavanini et al., 2006). Theoretically, glycine, taurine or β–alanine could mediate inhibition. However, taurine and β–alanine more commonly activate channels with long-duration bursts than glycine at extrasynaptic receptors. These results suggest that taurine and β–alanine may mediate slow synaptic inhibition and could have neurotransmitter roles in the VB nuclei. If the slow component results from the action of β–amino acids and not glycine, as suggested by Ghavanini et al. (2006), it seems likely that AMBD was specific for the synaptic actions of β–amino acids.

4.3.2 Intermediate and fast decay time constants

Our results showed that AMBD abolished the intermediate component and reduced the peak amplitude of the fast component of mixed IPSCs with fast and intermediate components. In the VB nuclei, the fast and slow components are attributable to glycine receptor activation, whereas the intermediate components are attributable to $GABA_A$ receptor activation (see also, Ghavanini et al., 2005; 2006). It is plausible that mixed IPSCs with fast and intermediate components were mediated by β–alanine rather than GABA, because β-alanine binds to both glycine and $GABA_A$ receptors (Wu et al., 1993). Based on this reasoning, our results imply that AMBD eliminated the intermediate component of mixed IPSCs, possibly due to specific antagonism of β–alanine-mediated inhibition, rather than antagonism of inhibition mediated by released GABA. In addition, our results show that AMBD reduced the peak amplitude of the fast component, suggesting some antagonism of fast glycinergic inhibition.

4.4 Presynaptic actions of AMBD

4.4.1 Spontaneous IPSCs

AMBD decreased the apparent frequency of sIPSCs with no effects on amplitude, suggesting a presynaptic effect (cf. Figure 3.16). Past studies on embryonic hippocampal neurons have indicated that sIPSCs largely result from the release of single synaptic vesicles (mono-quantal packets of neurotransmitter). A decrease in the frequency of sIPSCs after application of a pharmacological agent is expected from a presynaptic drug action on nerve terminal release, whereas a concomitant decrease in sIPSC amplitude indicates a postsynaptic action (Fatt and Katz, 1952; Vautrin et al., 1993). Kontro and

Oja (1987) found that AMBD attenuated K^+-stimulated taurine release in cerebral cortex. Hence, AMBD may have actions on nerve terminals or presynaptic neurons.

Although analysis of sIPSCs is powerful for the identification of presynaptic actions, it is not without ambiguities. Postsynaptic blockade of the glycine or $GABA_A$ receptors may produce a reduction in frequency of sIPSCs, without a presynaptic effect (cf. Vautrin et al., 1993). Although we propose that the observed decrease in sIPSC frequency results from a presynaptic effect on transmitter release, the decrease could have resulted from postsynaptic AMBD blockade.

4.4.2 Modulation of GABA release by the glycine receptor

Theoretically, AMBD-mediated blockade of a presynaptic site that attenuates GABA release from nerve terminals could decrease $GABA_A$ergic transmission, leading to reduction of isolated $GABA_A$ergic IPSCs. For example, studies on glycine and GABA co-release in the medial nucleus of the trapezoid body and spinal cord have shown that glycine activates presynaptic glycine receptors that increase the release of GABA (Jones, 1991; Turecek and Trussell, 2001). These and other studies (Malminen and Kontro, 1989) may suggest that glycine-like amino acids and taurine released from glia could modulate GABA release from nerve terminals.

In support of this possibility, our results show that AMBD reduced the peak amplitude of mixed IPSCs, as well as isolated glycinergic and $GABA_A$ergic IPSCs (cf. Figure 3.6 and Figure 3.8). Furthermore, AMBD had little effect on postsynaptic $GABA_A$ receptors (cf.

Figure 3.10). Given our observations of decreased frequency of sIPSCs, the present data imply that the effects of AMBD on isolated $GABA_A$ergic IPSCs may have resulted from actions on a presynaptic site that mediates GABA release from nerve terminals.

4.4.3 Co-release versus co-transmission

We did not observe a prevalence of bi-phasic sIPSCs expected from co-release of GABA and the glycine-like amino acids. Bi-phasic sIPSCs are associated with the release of two transmitters within single quanta that activate two channels with different kinetics. Neurons showing exclusively glycinergic or $GABA_A$ergic responses suggest co-transmission by independent pathways (cf. Donato and Nistri, 2000; Dumoulin et al., 2001; Ghavanini et al., 2006). In the VB nuclei, the provenance of released GABA and the glycine-like amino acids is likely from co-localized nerve terminals.

4.5 Proposed mechanism of AMBD antagonism

We propose that AMBD has both presynaptic and postsynaptic sites of action. Our results show that AMBD eliminated the slow component and reduced the peak amplitude of the fast component of mixed IPSCs and antagonized isolated and purely glycinergic IPSCs. We suggest that AMBD antagonized the actions of glycine-like transmitters at the postsynaptic receptor or receptors mediating fast and slow IPSCs. The glycine receptor mediating slow IPSCs may specifically bind β–amino acids, supporting the role of AMBD as an antagonist of a potential β–amino acid receptor. In addition, our results show that AMBD reduced the peak amplitude of isolated $GABA_A$ergic IPSCs with no effects on the majority of purely $GABA_A$ergic IPSCs and decreased the apparent

frequency of sIPSCs. We suggest that AMBD blocks a presynaptic site that normally increases spatially co-localized GABA release, thereby decreasing the amplitude of isolated GABA$_A$ergic IPSCs. Figure 4.1 depicts the proposed mechanism for AMBD antagonism.

4.6 Future directions

Studies on differential antagonism of extrasynaptic receptors activated by exogenous application of glycine-like amino acids and GABA may help to resolve whether AMBD is specific for particular agonist interactions at the GABA$_A$ receptor. Unfortunately, there may be substantial differences between synaptic and extrasynaptic receptors, such as Cl$^-$ permeability and conductance (Ghavanini et al., 2006). Synthesis and pharmacological studies of β–alanine analogues represent an important future approach.

Although *in vivo* studies of AMBD actions were not within the scope of this thesis, these experiments would provide insight into the potential neurotransmitter role of glycine-like amino acids. Injection of AMBD into live animals would further discriminate between the antagonistic actions of AMBD and strychnine, and potentially clarify the role of the β-amino acid receptor. Classical studies have shown that strychnine reduces the threshold for sensory evoked convulsions and induces allodynia *in vivo* (Sherrington, 1947), suggesting that glycinergic transmission plays an important role in sensory processing (cf. Ran et al., 2004). Determination of whether AMBD also reduces the threshold for sensory evoked convulsions could potentially provide evidence for the role of β–amino acids in sensory pathophysiology. The involvement of the thalamus in pain
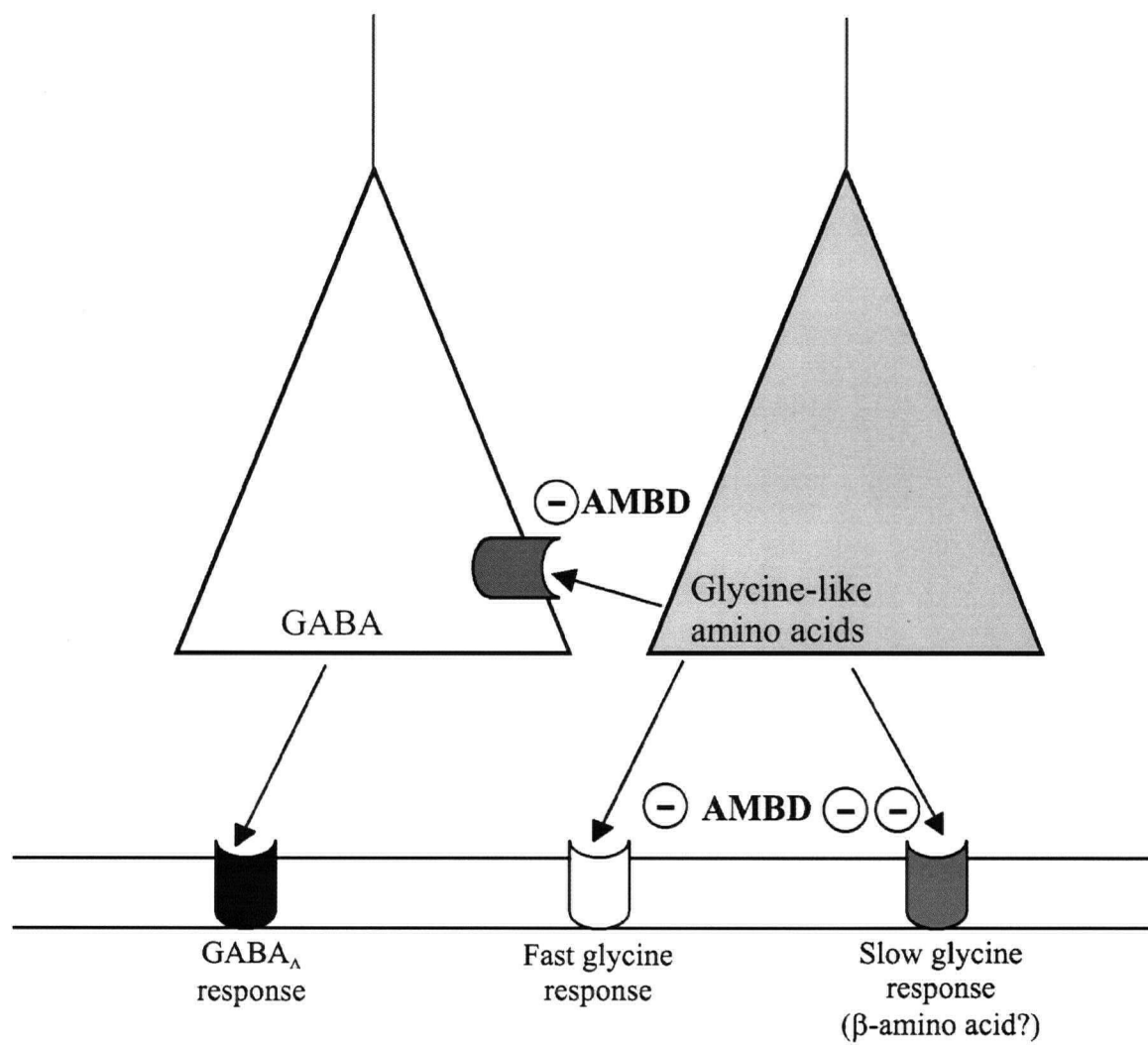
Figure 4.1 Proposed mechanism for AMBD antagonism.

transmission (Ohye, 1998), suggests that the characterization of β–amino acid receptor agonists antagonized by AMBD may help in the development of analgesic drugs (cf. Hornfeldt et al., 1992).

4.7 Conclusions

The major finding of these studies was that AMBD specifically antagonized the peak amplitude of mixed, isolated, and purely glycinergic IPSCs, but had little effect on purely GABA$_A$ergic IPSCs. Furthermore, AMBD abolished the slow and intermediate components of biexponentially fitted mixed IPSCs and decreased the frequency of sIPSCs, with no effects on their amplitude.

AMBD antagonism of IPSCs did not result from actions on passive or active membrane properties. Rather, AMBD-mediated IPSC reduction was a likely consequence of both postsynaptic and presynaptic effects. We propose that AMBD specifically antagonizes transmitter action at the postsynaptic glycine receptors that mediate fast and slow IPSCs. We raise this possibility from observations of specific AMBD-mediated elimination of the slow component of mixed IPSCs and reduction in the peak amplitude of the fast component. The postsynaptic glycine receptor that mediates slow IPSCs may be the potential β–amino acid receptor, although it has not been fully characterized. In addition, AMBD antagonized a presynaptic site, thereby modulating the release of GABA in spatially co-localized terminals. We base this possibility on our evidence that AMBD reduced isolated GABA$_A$ergic IPSC peak amplitude, with no effects on the majority of purely GABA$_A$ergic IPSCs and caused a decrease in sIPSC frequency.

References

Akers, R. M., Killackey, H. P., 1979. Segregation of cortical and trigeminal afferents to the ventrobasal complex of the neonatal rat. Brain Res. 161, 527-532.

Alitto, H. J., Usrey, W. M., 2003. Corticothalamic feedback and sensory processing. Curr. Opin. Neurobiol. 13, 440-445.

Araki, T., Yamano, M., Murakami, T., Wanaka, A., Betz., H., Tohyama, M., 1988. Localization of glycine receptors in the rat central nervous system: an immunohistochemical analysis using monoclonal antibody. Neurosci. 25, 613-624.

Ashcroft, F. M., Gribble, F. M., 2000. New windows on the mechanism of action of K_{ATP} channel openers. Trends Pharmacol. Sci. 21, 439-445.

Barakat, L., Wang, D., Bordey, A., 2002. Carrier-mediated uptake and release of taurine from Bergmann glia in rat cerebellar slices. J. Physiol. 541, 753-767.

Bartho, P., Freund, T. F., Acsady, L., 2002. Selective GABAergic innervation of thalamic nuclei from zona incerta. Eur. J. Neurosci. 16, 999-1014.

Beato, M., Groot-Kormelink, P. J., Colquhoun, D., Sivilotti, L. G., 2002. Openings of the rat recombinant $\alpha1$ homomeric glycine receptor as a function of the number of agonist molecules bound. J. Gen. Physiol. 119, 443-466.

Billard, J. M., Batini, C., 1991. Decreased sensitivity of cerebellar nuclei neurons to GABA and taurine: effects of long-term inferior olive destruction in the rat. Neurosci. Res. 9, 246-256.

Bohlhalter, S., Mohler, H., Fritschy, J. M., 1994. Inhibitory neurotransmission in rat spinal cord: co-localization of glycine and $GABA_A$ receptors at GABAergic synaptic contacts demonstrated by triple immunofluorescence staining. Brain Res 642, 59-69.

Bokor, H., Frere, S. G. A., Eyre, M. D., Slezia, A., Ulbert, I., Luthi, A., Acsady, L., 2005. Selective GABAergic control of higher-order thalamic relays. Neuron 45, 929-940.

Bormann, J., Rundstrom, N., Betz, H., Langosch, D., 1993. Residues within transmembrane segment M2 determine chloride conductance of glycine receptor homo- and hetero-oligomers. EMBO J. 12, 3729-3737.

Bormann, J., 2000. The 'ABC' of GABA receptors. Trends Pharmacol. Sci., 21, 16-19.

Bowery, N., 1989. $GABA_B$ receptors and their significance in mammalian pharmacology. Trends Pharmacol. Sci. 10, 401-407.

Castro-Alamancos, M. A., Calcognotto, M. E., 2001. High-pass filtering of corticothalamic activity by neuromodulators released in the thalamus during arousal: in vitro and in vivo. J. Neurophysiol. 85, 1489-1497.

Chaudhry, Reimer, R. J., Bellocchio, E. E., Danbolt, N. C., Osen, K. K., Edwards, R. H., 1998. The vesicular GABA transporter VGAT localizes to synaptic vesicles in sets of glyinergic as well as GABAergic neurons. J. Neurosci. 18, 9733-9750.

Cope, D. W., Hughes, S. W., Crunelli, V., 2005. GABA$_A$-receptor mediated tonic inhibition in thalamic neurons. J. Neurosci. 25, 11553-11563.

Corringer, P. J., Le Novere, N., Changeux, J. P., 2000. Nicotinic receptors at the amino acid level. Annu. Rev. Pharmacol. Toxicol. 40, 431-458.

Curtis, D. R., Hosli, L., Johnston, G. A., Johnston, I. H., 1968. The hyperpolarization of spinal motoneurons by glycine and related amino acids. Exp. Brain Res. 5, 235-258.

Curtis, D. R., Duggan, A. W., Felix, D., Johnston, G. A., McLennan, H., 1971. Antagonism between bicuculline and GABA in the cat brain. Brain Res. 33, 57-73.

Diamond, M. E., Armstrong-James, M., Budway, M. J., Ebner, F. F., 1992. Somatic sensory responses in the rostral sector of the posterior group (Pom) and in the ventral posterior medial nucleus (VPM) of the rat thalamus: dependence on the barrel field cortex. J. Comp. Neurol. 319, 66-84.

DiFrancesco, D., Tortora, P., 1991. Direct activation of cardiac pacemaker channels by intracellular cyclic AMP. Nature 351, 145-147.

Donato, R., Nistri, A., 2000. Relative contribution by GABA or glycine to Cl-mediated synaptic transmission on rat hypoglossal motoneurons in vitro. J. Neurophysiol. 84, 2715-2724.

Dumoulin, A., Rostaing, P., Bedet, C., Levi, S., Isambert, M. F., Henry, J. P., 1999. Presence of the vesicular inhibitory amino acid transporter in GABAergic and glycinergic synaptic terminal boutons. J. Cell Sci. 112, 811-823.

Dumoulin, A., Triller, A., Dieudonne, S., 2001. IPSC kinetics at identified GABAergic and mixed GABAergic and glycinergic synapses onto cerebellar Golgi cells. J. Neurosci. 21, 6045-6057.

Eulenburg, V., Armsen, W., Betz, H., Gomeza, J., 2005. Glycine transporters: essential regulators of neurotransmission. Trends Biochem. Sci. 30, 325-333.

Fatt, P., Katz, B., 1952. Spontaneous subthreshold activity at motor nerve endings. J. Physiol. 117, 109-128.

Feldman, S. G., Kruger, L., 1980. An axonal transport study of the ascending projection of medial lemniscal neurons in the rat. J. Comp. Neurol. 192, 427-454.

Frosini, M., Sesti, C., Dragoni, S., Valoti, M., Palmi, M., Dixon, H. B. F., Machetti, F., Sgaragli, G., 2003. Interactions of taurine and structurally related analogues with the GABAergic system and taurine binding sites of rabbit brain. Br. J. Pharmacol. 138, 1163-1171.

Frostholm, A., Rotter, A., 1985. Glycine receptor distribution in mouse CNS: autoradiographic localization of [^{3}H]strychnine binding sites. Br. Res. Bull. 15, 473-486.

Gatti, P. J., Souza, J. D., Namath, I. J., Da Silva, A. M., Holtman, J. R. Jr., Gillis, R., 1985. Comparative cardiorespiratory effects produced by taurine and glycine applied to the ventral surface of the medulla. J. Pharmacol. Exp. Ther. 235, 820-828.

Ghavanini, A. A., Mathers, D. A., Puil., E., 2005. Glycinergic inhibition in thalamus revealed by synaptic receptor blockade. Neuropharm. 49, 338-349.

Ghavanini, A. A., Mathers, D. A., Kim, H. S., Puil, E., 2006. Distinctive glycinergic currents with fast and slow kinetics in thalamus. J. Neurophysiol, Epub ahead of print.

Girard, Y., Atkinson, J. G., Haubrich, D. R., Williams, M., Yarbrough, G. G., 1982. Aminomethyl-1,2,4-benzothiadiazines as potential analogues of γ-aminobutyric acid. Unexpected discovery of a taurine antagonist. J. Med. Chem. 25, 113-116.

Graham, D., Pfeiffer, F., Betz, H., 1983. Photoaffinity labeling of the glycine receptor of rat spinal cord. Eur. J. Biochem. 131, 519-525.

Grillner, S. Ekeberg, E. L., Manira, A., Lansner, A., Parker, D., Tegner, J., 1998. Intrinsic function of a neuronal network – a vertebrate central pattern generator. Brain Res. Rev. 26, 184-197.

Guillery, R. W., Sherman, S. M., 2002. Thalamic relay functions and their role corticocortical communication: generalizations from the visual system. Neuron 33, 163-175.

Han, N. L. R., Haddrill, J. L., Lynch, J. W., 2001. Characterization of a glycine receptor domain that controls the binding and gating mechanisms of the β–amino acid agonist, taurine. J. Neurochem. 79, 636-647.

Harris, R. M., Hendrickson, A. E., 1987. Local circuit neurons in the rat ventrobasal thalamus – a GABA immunocytochemical study. Neurosci. 21, 229-236.

Harsing, L. G. J., Gacsalyi, I., Szabo, G., Schmidt, E., Sziray, N., Sebban, C., Tesolin-Decros, B., Matyus, P., Egyed, A., Spedding, M., Levay, G., 2003. The glycine

transporter-1 inhibitors NFPS and Org 24461: a pharmacological study. Pharmacol. Biochem. Behav. 74, 811-825.

Heaulme, M., Chambon, J. P., Leyris, R., Molimard, J. C., Wermuth, C. G., Biziere, K., 1986. Biochemical characterization of the interaction of three pyridazinyl-GABA derivatives with the $GABA_A$ receptor site. Brain Res. 384, 224-231.

Hirai, T., Jones, E. G., 1988. Segregation of lemniscal inputs and motor cortex outputs in cat ventral thalamic nuclei: application of a novel technique. Exp. Brain Res. 71, 329-344.

Hornfeldt, C. S., Smullin, D. H., Schamber, C. D., Sun, X., Larson, A. A., 1992. Antinociceptive effects of intrathecal taurine and calcium in the mouse. Life Sci. 50, 1925-1934.

Huguenard, J. R., Prince, D. A., 1994. Intrathalamic rhythmicity studied in vitro: nominal T-current modulation causes robust antioscillatory effects. J. Neurosci. 14, 5485-5502.

Huxtable, R. J., Laird, H. E., Lippincott, S. E., 1979. The transport of taurine in the heart and the rapid depletion of tissue taurine content by guanidinoethyl sulfonate. J. Pharmacol. Exp. Ther. 211, 465-471.

Huxtable, R. J., Franconi, F., Giotti, A., 1987. The biology of taurine. Advances of Experimental Medicine 217. Plenum Press, New York.

Huxtable, R. J., 1989. Taurine in the central nervous system and the mammalian actions of taurine. Prog. Neurobiol. 32, 471-533.

Ito, S., Cherubini, E., 1991. Strychnine-sensitive glycine responses of neonatal rat hippocampal neurons. J. Physiol. 440, 67-83.

Johnston, G. A., 1996. $GABA_A$ receptor pharmacology. Pharmacol. Ther. 69, 173-198.

Jonas, P., Bischofberger, J., Sandkuhler, J., 1998. Corelease of two fast neurotransmitters at a central synapse. Science 281, 360-361.

Jones, E. G., 1991. The anatomy of sensory relay functions in the thalamus. Prog. Brain Res. 87, 29-52.

Jursky, F., Nelson, N., 1995. Localization of glycine neurotransmitter transporter (GLYT2) reveals correlation with the distribution of glycine receptor. J. Neurochem. 64, 1026-1033.

Kaczmarek, L. K., 1976. A comparison of the evidence for taurine and GABA as neurotransmitters. In: Taurine, edited by Huxtable, R., Barbeau, A.. New York: Raven, 283-292.

Kaila, K., 1994. Ionic basis of $GABA_A$ receptor channel function in the nervous system. Prog. Neurobiol. 42, 489-537.

Kirkpatrick, F. H., Sandberg, H. E., 1973. Effects of preparation method on reversible conformational changes induced by neutral salts in spin-labeled erythrocyte membranes. Arch. Biochem. Biophys. 156, 653-657.

Kirsch, J., Betz, H., 1995. The postsynaptic localization of the glycine receptor-associated protein gephyrin is regulated by the cytoskeleton. J. Neurosci. 15, 4148-4156.

Kontro, P., Oja, S. S., 1983. Sodium-independent taurine binding to brain synaptic membranes. Cell Mol. Neurobiol. 3, 183-187.

Kontro, P., Korpi, E. R., Oja, O. S., Oja, S. S., 1984. Modulation of noradrenaline uptake and release by taurine in rat cerebral slices. Neuroscience 13, 663-666.

Kontro, P., Oja, S. S., 1987. Taurine and GABA release from mouse cerebral cortex slices: effects of structural analogues and drugs. Neurochem. Res. 12, 475-482.

Kuhse, J., Schmeiden, V., Betz, H., 1990. Identification and functional expression of a novel ligand binding subunit of the inhibitory glycine receptor. J. Biol. Chem. 265, 22317-22320.

Kurachi, M., Aihara, H., 1985. The action of taurine on the response to glutamate in the motoneuron of the isolated frog spinal cord. Neuropharmacology 24, 775-781.

Legendre, P., 2001. The glycinergic inhibitory synapse. Cellular and Molecular Life Sciences 58, 760-793.

Lewin, L., Rassin, D. K., Sellstrom, A., 1994. Net taurine transport and its inhibition by a taurine antagonist. Neurochem. Res. 19, 347-352.

Li, Y., Wu, L. J., Legendre, P., Xu, T. L., 2003. Asymetric cross-inhibition between $GABA_A$ and glycine receptors in rat spinal dorsal horn neurons. J. Biol. Chem. 278, 38637-38645.

Liu, Q. R., Lopez-Corcuera, B., Nelson, H., Mandiyan, S., Nelson, N., 1992. Cloning and expression of a cDNA encoding the transporter of taurine and β-alanine in mouse brain. Proc. Nat. Acad. Sci. USA 89, 12145-12149.

Lynch, J. W., Rajendra, S., Barry, P. H., Schofield, P.R., 1995. Mutations affecting the glycine receptor agonist transduction mechanism convert the competitive antagonist, picrotoxin, into an allosteric potentiator. J. Biol. Chem. 270, 13799-13806.

Lynch, J. W., 2004. Molecular structure and function of the glycine receptor chloride channel. Physiol. Rev. 84, 1051-1095.

MacDonald, R. L., Olsen, R. W., 1994. $GABA_A$ receptor channels. Annu. Rev. Neurosci. 17, 569-602.

Maksay, G., Ticku, M. K., 1984. Diazotization and thiocyanate differentiate agonists from antagonists for the high- and low-affinity receptors of γ–aminobutyric acid. J. Neurochem 43, 261-268.

Malminen, O, Kontro, P., 1989. Gamma-aminobutyric acid and benzodiazepine receptors in cultured cerebellar granule cells: effects of taurine and its lipophilic derivatives. Neuropharmacology 28, 907-912.

Malosio, M. L., Marqueze-Pouey, B., Kuhse, J., Betz, H., 1991. Widespread expression of glycine receptor subunit mRNAs in the adult and developing rat brain. EMBO Journal 10, 2401-2409.

Manson, J. R. M., 1969. The somatosensory cortical projection of single nerve cells in the thalamus of the cat. Brain Res. 12, 489-492.

Martin, G. E., Bendesky, R. J., Williams, M., 1981. Further evidence for selective antagonism of taurine by 6-aminomethyl-3-methyl-4H-1,2,4-benzothiadiazine-1,1-dioxide. Brain Res. 299, 530-535.

Mathers, D. A., 1993. Effects of the benzothiadiazine TAG on channel activation at mammalian glycine receptors. Neurosci. Lett. 149, 23-26.

Mayer, M. L., 1981. Inhibitory actions of amino acids in the preoptic-anterior hypothalamus of the rat. Exp. Brain Res. 43, 154-158.

McCormick, D. A., 1989. Cholinergic and noradrenergic modulation of thalamocortical processing. Trends Neurosci. 12, 215-221.

McCormick, D. A., Pape, H. C., 1990. Properties of a hyperpolarization-activated cation current and its role in rhythmic oscillation in thalamic relay neurones. J. Physiol. 431, 291-318.

Michaud, J. C., Mienville, J. M., Chambon, J. P., Biziere, K., 1986. Interactions between three pyridazinyl-GABA derivatives and central GABA and glycine receptors in the rat, an in-vitro microionophoretic study. Neuropharm. 25, 1197-1203.

Mori, M., Gahwiler, B. H., Gerber, U., 2002. β–alanine and taurine as endogenous agonists at glycine receptors in rat hippocampus in vitro. J. Physiol. 539, 191-200.

Mountcastle, V. B., Poggio, G. F., Werner, G., 1963. The relation of thalamic cell response to peripheral stimuli varied over an intensive continuum. J. Neurophysiol. 26, 807-834.

Nayeem, N., Green, T. P., Martin, I. L., Barnard, E. A., 1994. Quaternary structure of the native $GABA_A$ receptor determined by electron microscopic image analysis. J. Neurochem. 62, 815-818.

Nelson, N., 1998. The family of Na^+/Cl^- neurotransmitter transporters. J. Neurochem. 71, 1785-1803.

Nunez, E., Lopez-Corcuera, B., Vazquez, J., Gimenez, C., Aragon, C., 2000. Differential effects of the tricyclic antidepressant amoxapine on glycine uptake mediated by the recombinant GlyT1 and GlyT2 glycine transporters. Br. J. Pharmacol. 129, 200-206.

Ohye, C., 1998. Stereotactic treatment of central pain. Stereotact. Funct. Neurosurg. 70, 71-76.

Okamoto, K., Kimura, H., Sakai, Y., 1983. Evidence for taurine as an inhibitory neurotransmitter in cerebellar stellate interneurons: selective antagonism by TAG (6-aminomethyl-3-methyl-4H,1,2,4-benzothiadiazine-1,1-dioxide). Brain Res. 265, 163-168.

Padjen, A. L., Mitsoglou, G. M., Hassessian, H., 1989. Further evidence in support of taurine as a mediator of synaptic transmission in the frog spinal cord. Brain Res. 488, 288-296.

Pan, Z. H., Slaughter, M. M., 1995. Comparison of the actions of glycine and related amino acids on isolated third order neurons from the tiger salamander retina. Neurosci. 64, 153-164.

Peschanski, M., Ralston, H. J., Roudier, F., 1983. Reticularis thalami afferents to the ventrobasal complex of the rat thalamus; an electron microscope study. Brain Res. 270, 325-329.

Pow, D. V., Sullivan, R., Reye, P., Hermanussen, S., 2002. Localization of taurine transporters, taurine and (3)H taurine accumulation in the rat retina, pituitary and brain. Glia 37, 153-168.

Rajendra, S., Vandenberg, R. J., Pierce, K. D., Cunningham, A. M., French, P. W., Barry, P. H., Schofield, P. R., 1995. The unique extracellular disulphide loop of the glycine receptor is a principle ligand binding element. EMBO J. 14, 2987-2998.

Rampon, C., Luppi, P. H., Fort, P., Peyron, C., Jouvet, M., 1996. Distribution of glycine-immunoreactive cell bodies and fibers in the rat brain. Neurosci. 75, 737-755.

Ran, I., Mathers, D. A., Puil, E., 2004. Pentobarbital induces thalamic oscillations in brain slices, modulated by GABA and glycine receptors. Neuropharmacology 47, 985-993.

Ries, C. R., Puil, E., 1999. Mechanism of anesthesia revealed by shunting actions of isoflurane on thalamocortical neurons. J. Neurophysiol. 81, 1795-1801.

Roux, M. J., Supplisson, S., 2000. Neuronal and glial glycine transporters have different stoichiometries. Neuron 25, 373-383.

Ruiz-Gomez, A., Morato, E., Garcia-Calvo, M., Valdivieso, F., Mayor, F. J., 1990. Localization of the strychnine binding site on the 48-kilodalton subunit of the glycine receptor. Biochem. 29, 7033-7040.

Sherrington C., 1947. Coordination in the simple reflex. The Integrative Action of the Nervous System. Yale University Press, New Haven, 107-114.

Shirasaki, T., Klee, M. R., Nakaye, T., Akaike, N., 1991. Differential blockade of bicuculline and strychnine on GABA- and glycine-induced responses in dissociated rat hippocampal pyramidal cells. Brain Res. 561, 77-83.

Sigel, E., Baur, R., Kellenberger, S., Malherbe, P., 1992. Point mutations affecting antagonist affinity and agonist dependent gating of $GABA_A$ receptor channels. EMBO J. 11, 2017-2023.

Simon, J., Wakimoto, H., Fujita, N., Lalande, M., Barnard, E. A., 2004. Analysis of the set of $GABA_A$ receptor genes in the human genome. J. Biol. Chem. 279, 41422-41435.

Smith, K. E., Borden, L. A., Wang, C. H., Hartig, P. R., Branchek, T. A., Weinshank, R. L., 1992. Cloning and expression of a high-affinity taurine transporter from rat brain. Mol. Pharmacol. 42, 563-569.

Steriade, M., 2005. Sleep, epilepsy and thalamic reticular inhibitory neurons. Trends Neurosci. 28, 317-324.

Tokutomi, N., Kaneda, M., Akaike, N., 1989. What confers specificity on glycine for its receptor site? Br. J. Pharmacol. 97, 353-360.

Turecek, R., Trussell, L. O., 2001. Presynaptic glycine receptors enhance transmitter release at a mammalian central synapse. Nature 411, 587-590.

Turner, J. P., Anderson, C. M., Williams, S. R., Crunelli, V., 1997. Morphology and membrane properties of neurones in the cat ventrobasal thalamus in vitro. J. Physiol. 505, 707-726.

Vafa, B., Lewis, T. M., Cunningham, A. C., Jacques, P., Lynch, J. W., Schofield, P. R., 1999. Identification of a new ligand binding domain in the α1 subunit of the inhibitory glycine receptor. J. Neurochem. 73, 2158-2166.

Vautrin, J., Schaffner, A. E., Fontas, B., Barker, J. L., 1993. Frequency modulation of transmitter release. J. Physiol. Paris 87, 51-73.

Waite, P. M., 1973. Somatotopic organization of vibrissal responses in the ventrobasal complex of the rat thalamus. J. Physiol. 228, 527-540.

Wan, X., Puil, E., 2002. Pentobarbital depressant effects are independent of GABA receptors in auditory thalamic neurons. J. Neurophysiol. 88, 3067-3077.

Ward, R., Danzinger, S., Owen, V., Rafal, R., 2002. Deficits in spatial coding and feature binding following damage to spatiotopic maps in the human pulvinar. Nat. Neurosci. 5, 99-100.

Welker, W. I., 1973. Principles of organization of the ventrobasal complex in mammals. Brain, Behav. Evol. 7, 253-336.

Werman, R., Davidoff, R. A., Aprison, M. H., 1968. Inhibitory action of glycine on spinal neurons of the cat. J. Neurophysiol. 31, 81-95.

Wessberg, P., Hedner, T., Hedner, J., Jonason, J., 1983. Effects of taurine and a taurine antagonist on some respiratory and cardiovascular parameters. Life Sci. 33, 1649-1655.

Womack, M., Khodakhah, K., 2002. Active contribution of dendrites to the tonic and trimodal patterns of activity in cerebellar Purkinje neurons. J. Neurosci. 22, 10603-10612.

Wu, F. S., Gibbs, T. T., Farb, D. H., 1993. Dual activation of GABA and glycine receptors by beta-alanine; inverse modulation by progesterone and 5-alpha-pregnan-3 alpha-ol-20-one. Eur. J. Pharmacol. 246, 239-246.

Yarbrough, G. G., Singh, D. K., Taylor, D. A., 1981. Neuropharmacological characterization of a taurine antagonist. J. Pharmacol. Exp. Ther. 219, 604-613.

Yen, C. T., Jones, E. G., 1983. Intracellular staining of physiologically identified neurons and axons in the somatosensory thalamus of the cat. Brain Res. 280, 148-154.

Yen, C. T., Conley, M., Jones, E. G., 1985. Morphological and functional types of neurons in cat ventral posterior thalamic nucleus. J. Neurosci. 5, 1316-1338.

Zarbin, M. A., Wamsley, J. K., Kuhar, M. J., 1981. Glycine receptor: light microscopic autoradiographic localization with [^{3}H]strychnine. J. Neurosci. 1, 532-547.

Zeilhofer, H. U., Studler, B., Arabadzisz, D., Schweizer, C., Ahmadi, S., Layh, B., Bosl, M. R., Fritschy, J. M., 2005. Glycinergic neurons expressing enhanced green fluorescent protein in bacterial artificial chromosome transgenic mice. J. Comp. Neurol. 482, 123-141.

Zhao, P., Huang, Y. L., Cheng, J. S., 1999. Taurine antagonizes calcium overload induced by glutamate or chemical hypoxia in cultured rat hippocampal neurons. Neurosci. Lett. 268, 25-28.